Interstellar Medium (ISM)

Lecture 11
2025 May 12 (Monday), 9AM

updated 03/03, 17:47

선광일 (Kwangil Seon)
KASI / UST

Effects of Supernovae on the ISM

- Consider the simplest case of a spherically symmetric explosion of a star in a uniform density and temperature.
- ***Free-Expansion Phase***
  - Typical supernovae (SNe) explosion ejects a kinetic energy of

$$E_{51} \equiv E_0/(10^{51}\,\mathrm{erg}) \approx 1$$

$M_{\rm ej} \sim 10\,M_\odot$ for core collapse supernovae (Type II, Type Ib, and Type Ic), powered by the gravitational collapse of the dense core of an evolved massive star.
$M_{\rm ej} \sim 1\,M_\odot$ for the thermonuclear explosion of a white dwarf (Type Ia)

An explosion produces an energy $\sim 10^{53}\,\mathrm{erg}$ in neutrinos and $\sim 10^{49}$ erg in photons. These energies are not effectively deposited in the ISM.

  - The ejecta mass ranges from $M_{\rm ej} \sim 1.4\,M_\odot$ (Type Ia, white dwarf) to $M_{\rm ej} \sim 10 - 20\,M_\odot$ (Type II, core collapse of massive stars).
  - The ejecta will have a root-mean-square (rms) velocity of

$$v_{\rm ej} = \left(\frac{2E_0}{M_{\rm ej}}\right)^{1/2} = 1.00 \times 10^4\,\mathrm{km\,s^{-1}}\,E_{51}^{1/2}\left(\frac{M_{\rm ej}}{M_\odot}\right)^{-1/2}$$

$$\mathcal{M}_1 = \frac{v_{\rm ej}}{c_1} \approx \frac{1\times10^4\,\mathrm{km/s}}{1\,\mathrm{km/s}} \gg 1$$

    - This velocity is far greater than the sound speed in the surrounding material, and the expanding ejecta will drive a fast shock into the circumstellar medium.
  - All of the matter interior to this shock surface is referred to as the ***supernova remnant*** (SNR).
  - **The density of the ejecta far exceeds the density of the circumstellar medium**, and the ejecta continue to **expand ballistically at nearly constant velocity**. — this is referred to as the “free expansion phase.” The ejecta are not slowed down significantly until they have swept up a mass of interstellar gas comparable to the mass of the ejecta.

- At the early times of the free-expanding phase, there is only one shock, which propagating outward into the ambient medium.
- *As the ejecta expands, its density drops and less hot, thanks to adiabatic cooling. Then, the pressure ($P_2 \approx \mathscr{M}_1^2 P_1$) of the shocked circumstellar/interstellar medium soon exceeds the thermal pressure in the ejecta.*

$$\rho_{\rm ej} = \frac{M_{\rm ej}}{(4\pi/3)R^3} = \frac{M_{\rm ej}}{(4\pi/3)(v_{\rm ej}t)^3} \propto t^{-3}$$

  - As the pressure in the ejecta drops, a reverse shock is driven into the ejecta. The SNR now contains two shocks: the ***original outward-propagating shock*** (the blastwave) and the ***reverse shock propagating inward***, slowing and shock-heating the ejecta (which had previously been cooled adiabatic expansion).

- ***End of the free-expanding phase***: ***The reverse shock becomes important when the expanding ejecta material has swept up a mass of circumstellar or interstellar matter comparable to the ejecta mass.***
  - The radius of the blastwave and the time when this occurs are:

$$R_1 = \left(\frac{M_{\rm ej}}{(4\pi/3)\rho_0}\right)^{1/3} = 5.88\times10^{18}\,{\rm cm}\left(\frac{M_{\rm ej}}{M_\odot}\right)^{1/3} n_0^{-1/3}$$

$$t_1 \approx \frac{R_1}{v_{\rm ej}} = 186\,{\rm yr}\left(\frac{M_{\rm ej}}{M_\odot}\right)^{5/6} E_{51}^{-1/2} n_0^{-1/3}$$

$$R_1 = 0.525\,{\rm pc}\,(M_{\rm ej}/M_\odot)^{1/3}\, n_0^{-1/3}$$

$\rho_0 \simeq 1.4 m_{\rm p} n_0 \rightarrow$ density of the ambient (neutral) medium

$n_0 \rightarrow$ number density of hydrogen in the ambient medium

  - The free-expansion phase applies only for $t \lesssim t_1$.

- ***Sedov-Taylor Phase (Energy-Conserving Phase, Adiabatic Phase)***
  - For $t \gtrsim t_1$, the reverse shock has reached the center of the remnant, all of the ejecta are now very hot, and the free-expansion phase is over.
    - The pressure in the SNR is far higher than the pressure in the surrounding medium.
    - The hot gas may have been emitting radiation, but if the density is low, the radiative losses at early times are negligible.
    - We can idealize the explosion as a large amount of energy released instantaneously at a point **(blast wave)**, in the form of kinetic energy plus radiation.
  - The mass of shocked gas is much greater than the ejecta mass. The pressure P_2 behind the shock is much greater than the pressure P_1 of the surrounding gas. Hence, the properties of the shock front no longer depend on the ejecta mass and the surrounding gas pressure. The shock expands as if it were traveling into a pressureless medium.
  - The SNR now enters a phase where
    - We can neglect (1) the mass of the ejecta ($M_{\rm ej} \ll (4\pi/3)R^3\rho_0$), (2) radiative losses, and (3) the pressure in the ambient medium.
    - ***The shock front properties depend only on the energy of explosion E and the density ρ_0 of the ambient medium.***
    - This phase can be approximated by idealizing the problem as ***a "point explosion" injecting only energy E_0 (zero ejecta mass) into a uniform-density zero-temperature medium of density ρ_0, as in nuclear explosion.***

- ***Self-similar Solution***: In this phase, only the scale of the pressure and the length scale evolve with time, but the shape of the pressure and density as a function of position remains unaltered. These motions are called self-similar.
- The evolution during this phase is determined only by ***the energy of explosion*** E_0***, the density of interstellar gas*** ρ_0***, and the elapsed time from the explosion t***.

  We do simple dimensional analysis to find out the form of the time evolution of the remnant. Let the explosion occur at $t = 0$ and the radius of the shock front be R_s. Suppose that

E = [mass]x[length]^2/[time]^2
ρ = [mass]/[length]^3

$$R_s = AE^{\alpha}\rho_0^{\beta}t^{\eta} \qquad (A = \text{a dimensionless constant})$$

- By equating the powers of mass, length, and time, we obtain

$$\begin{aligned} \text{mass} &: 0 = \alpha + \beta \\ \text{length} &: 1 = 2\alpha - 3\beta \\ \text{time} &: 0 = -2\alpha + \eta \end{aligned} \longrightarrow \alpha = 1/5,\ \beta = -1/5,\ \eta = 2/5$$

- Then, the solution for the shock-front radius is given by

$$R_s = A\left(\frac{Et^2}{\rho_0}\right)^{1/5} \qquad A = 1.15167 \text{ for } \gamma = 5/3$$

for a monatomic gas.
This value is obtained from the exact solution.

- The solution gives ***the radius and velocity of the shock front***, and ***temperature of the post-shock gas:***

$$R_s = 1.54 \times 10^{19}\,[\mathrm{cm}]\, E_{51}^{1/5} n_0^{-1/5} t_3^{2/5}$$
$$V_s = 1950\,[\mathrm{km\,s^{-1}}]\, E_{51}^{1/5} n_0^{-1/5} t_3^{-3/5}$$
$$T_s = 5.25 \times 10^{7}\,[\mathrm{K}]\, E_{51}^{2/5} n_0^{-2/5} t_3^{-6/5}$$

$1.54 \times 10^{19}\,\mathrm{cm} = 5\,\mathrm{pc}$

$t_3 \equiv t/10^3\,\mathrm{yr}$

$V_s \equiv \dfrac{dR_s}{dt} = \dfrac{2}{5} A E^{1/5} \rho_0^{-1/5} t^{-3/5}$

$T_s = \dfrac{3}{16} m V_s^2 / k \quad \left(m \simeq \dfrac{1.4}{2.3} m_p\right) \quad \rho_0 = m n_0$

m = mass per particle in the fully ionized, post-shock region.

- We have been assuming that the internal structure of the remnant is given by a similarity solution: by this we mean that the density, velocity, and pressure can be written

$$\rho(r) = \rho_0 f(x)$$
$$v(r) = \frac{R_s}{t} g(x)$$
$$P(r) = \frac{\rho_0 R_s^2}{t^2} h(x)$$

$$x \equiv \frac{r}{R_s}$$

$f(x), g(x), h(x)$ are dimensionless functions.

Inserting these into the fluid equations, with the Rankine-Hugonit relations for boundary conditions,Taylor (1950) and Sedov (1959) found the solution for the dimensionless functions [f(x), g(x), h(x), and A] independently, in connection with the development of nuclear weapons.

- ***Alternative approach***:
  - For the strong shock, the specific internal (thermal) and the kinetic energies just behind the strong shock are given by, respectively:

$$\epsilon_{\rm int} = \epsilon_{\rm kin} = \frac{9}{32} V_s^2$$

  - Since the blast wave is slowing down with time, the specific energy of the internal gas varies with radius within the bubble of hot gas.
  - Provided that most of the mass in the supernova remnant is made up of shocked interstellar gas and the mass of the stellar eject can be neglected, the total energy in the bubble of hot gas E_0, which is equal to the energy injected by the supernova explosion since the radiative losses are negligible, is therefore

$$\begin{aligned} E_0 &= \phi \frac{4\pi}{3} R^3 \rho_0 \left(\epsilon_{\rm int} + \epsilon_{\rm kin}\right) \\ &= \phi \frac{3\pi}{4} R^3 \rho_0 \left(\frac{dR}{dt}\right)^2 \end{aligned}$$

ρ_0 = density of ambient medium
R = the radius of the shock front at time t

where ϕ is a structure parameter, a numerical factor of order unity which accounts for the radial dependence of specific energy within the bubble. This equation represents the equation of motion of the shock front.

$$R = \left(\frac{25}{3\pi\phi}\right)^{1/5} \left(\frac{E_0 t^2}{\rho_0}\right)^{1/5} \qquad A \equiv \left(\frac{25}{3\pi\phi}\right)^{1/5} = 1.15167 \text{ for } \gamma = 5/3$$

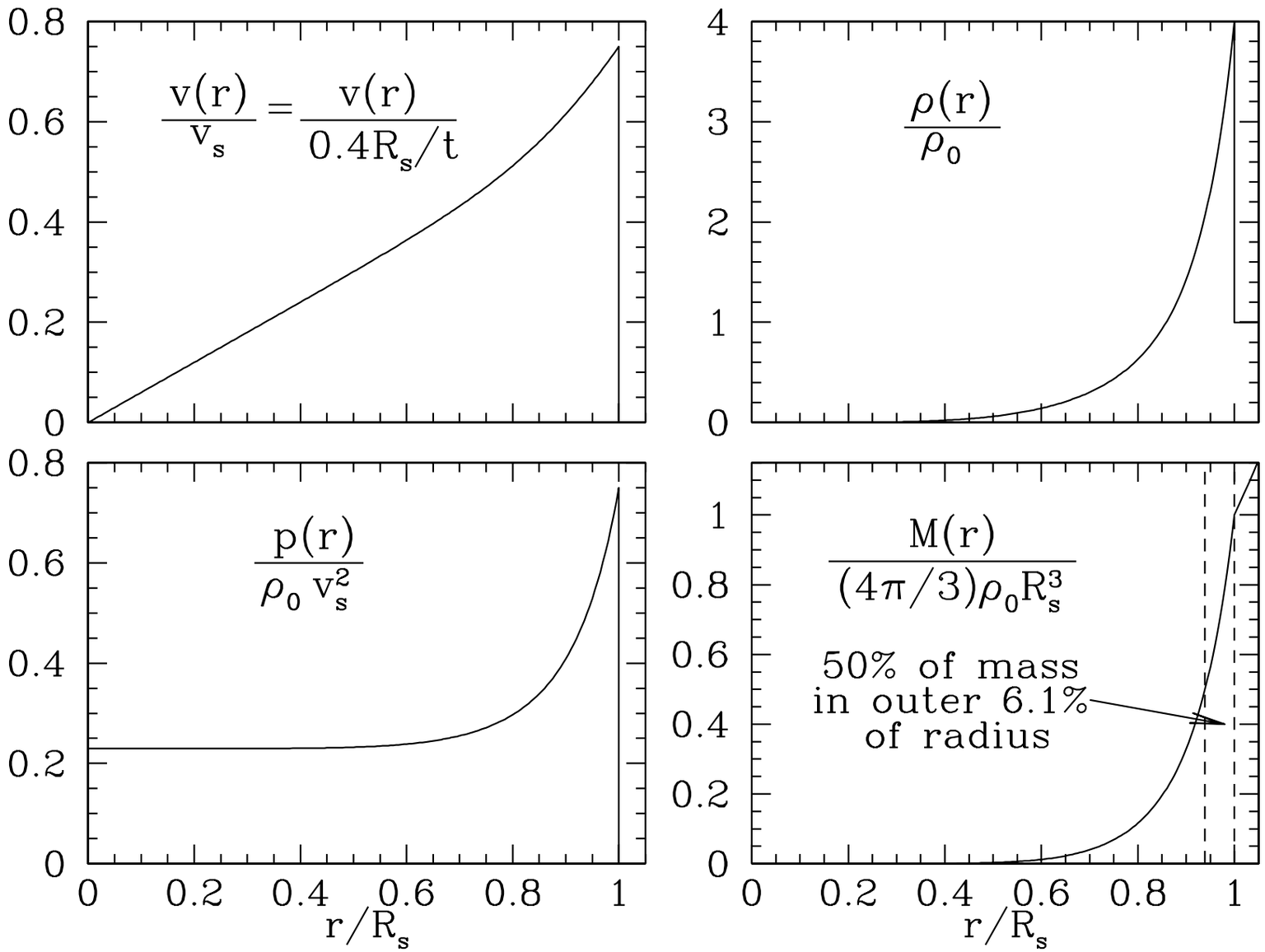

as $r \to 0$

$\rho(r)/\rho_0 \to 0$

$T(r)/T_s \to \infty$

$P(r)/P_0 \to 0.306$

Sedov-Taylor solution for γ = 5/3.

The temperature profile (not shown) can be obtained from the ratio of the pressure and density profiles. ***The density falls inward, and the temperature rises inward.***

[Figure 39.1, Draine]

- *End of the Sedov-Taylor phase*

- The hot gas interior to the shock front is, of course, radiating energy. When the radiative losses become important, a dense shell forms behind the shok and the SNR will leave the Sedov-Taylor phase and enter a "radiative" phase. In the radiative phase, the gas in the shell just interior to the shock front is now able to cool to temperatures much lower than the temperature $T_s = (3/16)mV_s^2/k$ at the shock front.
- In order to calculate the time scale, we need to estimate the cooling rate:

cooling function at a radius *r*:

$$\Lambda(r) \approx C\left[T(r)/10^6\,\mathrm{K}\right]^{-0.7} n_{\mathrm{H}}(r) n_e(r), \quad C = 1.1\times10^{-22}\,\mathrm{erg\,cm^3\,s^{-1}}, \quad n_e \simeq 1.2 n_{\mathrm{H}}$$

cooling rate at a time t, integrated over the volume of the SNR:

$$\frac{dE}{dt} = -\int_0^{R_s} \Lambda(r) 4\pi r^2 dr \qquad \longleftarrow \qquad n_{\mathrm{H}} n_e = 1.2 n_{\mathrm{H}}^2 = 1.2 n_0^2 \left[\rho(r)/\rho_0(r)\right]^2$$

$$= -1.2 C n_0^2 \left(T_s/10^6\,\mathrm{K}\right)^{-0.7} \frac{4\pi}{3} R_s^3 \left\langle (\rho/\rho_0)^2 (T_s/T)^{0.7} \right\rangle$$

Here, $n_0 \equiv n_{\mathrm{H}}(r = R_s)$ is the hydrogen density of the ambient medium at r = R_s.

$T_s \equiv T(r = R_s)$ is the temperature of the post-shock region at r = R_s.

$\langle \cdots \rangle$ denotes a volume-weighted average over the SNR.

From the Sedov-Taylor solution, we obtain $\left\langle (\rho/\rho_0)^2 (T_s/T)^{0.7} \right\rangle = 1.817$.

- Now, integrate the energy loss rate over a time interval *t* :

$$\Delta E(t) = -1.2 \times (1.817) C \frac{4\pi}{3} n_0^2 \int_0^t dt R_s^3 (T_s/10^6\,\mathrm{K})^{-0.7}$$

Using the previous solutions, we obtain the fractional energy loss by time *t* :

$$R_s = 1.54 \times 10^{19}\,[\mathrm{cm}]\, E_{51}^{1/5} n_0^{-1/5} t_3^{2/5}$$
$$T_s = 5.25 \times 10^{7}\,[\mathrm{K}]\, E_{51}^{2/5} n_0^{-2/5} t_3^{-6/5}$$

$$\frac{\Delta E(t)}{E_0} \approx -2.38 \times 10^{-6}\, n_0^{1.68} E_{51}^{-0.68} t_3^{3.04}$$

- If we suppose that the SNR enter the “radiative phase” when

$$\Delta E(t_{\mathrm{rad}})/E_0 \approx -1/3$$

we can solve for the cooling time t_{rad} :

$$t_{\mathrm{rad}} = 49.3 \times 10^3\,[\mathrm{yr}]\, E_{51}^{0.22} n_0^{-0.55}$$ end of the Sedov-Taylor phase

- The radius and shock speed at the end of the Sedov-Taylor phase are:

$$7.32 \times 10^{19}\,\mathrm{cm} = 23.7\,\mathrm{pc}$$

$$R_s(t_{\mathrm{rad}}) = 7.32 \times 10^{19}\,[\mathrm{cm}]\, E_{51}^{0.29} n_0^{-0.42}$$
$$V_s(t_{\mathrm{rad}}) = 188\,[\mathrm{km\,s^{-1}}]\, \left(E_{51} n_0^2\right)^{0.07}$$

Post-shock temperature is:

$$T_s(t_{\mathrm{rad}}) = 4.86 \times 10^5\,[\mathrm{K}]\, \left(E_{51} n_0^2\right)^{0.13}$$
$$kT_s(t_{\mathrm{rad}}) = 41\,[\mathrm{eV}]\, \left(E_{51} n_0^2\right)^{0.13}$$

- ***Snowplow Phase (Radiative Phase)***
  - At $t \approx t_{\rm rad}$
    - Cooling cause the thermal pressure just behind the shock to drop suddenly, and the shock wave briefly stalls. However, ***the very hot gas in the interior of the SNR has not cooled***.
    - The SNR now enters the snowplow phase, with a dense shell of cool gas enclosing a hot central volume where radiative cooling is unimportant.
    - This is called the snowplow phase because the expanding dense shell scoops up additional mass as it expands (the mass of the dense shell increases as it “sweeps up” the ambient gas). Since the gas cools well the shell will be thin and so the gas in the shell has a radial velocity that is almost the same as the shock front speed.
    - Most of the mass of a supernova remnant in the snowplow phase is in the dense shell. The inner region contains gas at very high temperatures. Thus, despite its low density, the gas in the inner region has a significant pressure, which push the dense shell outward.
    - The gas in the hot center cools by adiabatic expansion, and thus the pressure is given by

$$P \propto V^{-\gamma} \propto R_s^{-3\gamma} = R_s^{-5}$$

    - So that the pressure in the interior evolves as

$$P_i = P_0(t_{\rm rad}) \left(\frac{R_{\rm rad}}{R_s} \right)^5$$

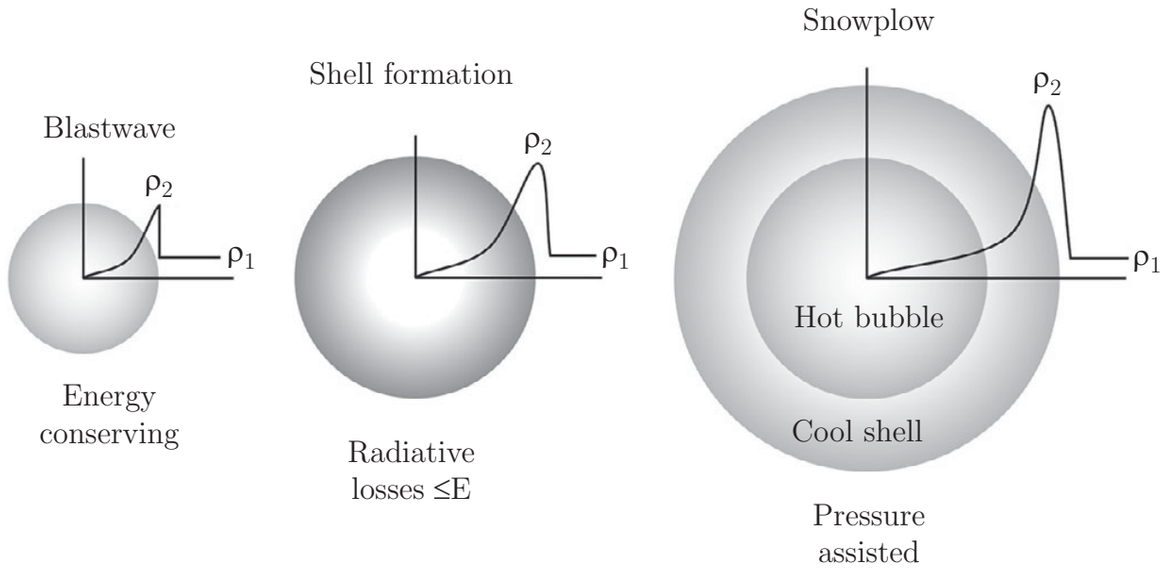

Transition from the Sedov-Taylor phase to the snowplow phase [Figure 5.5, Ryden]

- In the initial phase, the pressure exerted by the hot center causes the “radial momentum” of the shell to increases:

M_s = mass of the shell = mass of the ambient medium swept by the SNR

$$\frac{d}{dt}\left(M_s V_s\right) \approx P_i 4\pi R_s^2 = 4\pi P_0(t_{\rm rad}) R_{\rm rad}^5 R_s^{-3}$$

$$M_s = \left(\frac{4\pi}{3} R_s^3\right)\rho_0 \qquad V_s = \frac{dR_s}{dt} \longrightarrow \frac{d}{dt}\left(R_s^3 \frac{dR_s}{dt}\right) \propto R_s^{-3}$$

Suppose that there is a power-law solution:

$$R_s \propto t^\eta$$

$$4\eta - 2 = -3\eta \;\Rightarrow\; \eta = 2/7$$

$$R_s \approx R_s(t_{\rm rad})\,(t/t_{\rm rad})^{2/7}$$

$$V_s \approx \frac{2}{7}\frac{R_s}{t} = \frac{2}{7}\frac{R_s(t_{\rm rad})}{t_{\rm rad}}\left(\frac{t}{t_{\rm rad}}\right)^{-5/7}$$

- Because the effect of the internal pressure has been included, this solution is referred to as the ***pressure-modified (or pressure-driven) snowplow phase***.
- Note that with this construction, $R_s(t)$ is continuous from the Sedov-Taylor phase to the pressure-modified snowplow phase, but $V_s(t)$ undergoes a discontinuous drop by 2/7 ~ 29% at $t = t_{\rm rad}$.

- In the late phase of evolution, the stored thermal energy in the central region has been entirely radiated away, and only the momentum of the dense shell keeps the remnant expanding into the ISM.

$$\frac{d}{dt}\left(M_s V_s\right) = 0 \qquad M_s = \text{mass of the shell}$$

$$M_s = \left(\frac{4\pi}{3} R_s^3\right) \rho_0$$

$$V_s = \frac{dR_s}{dt} \longrightarrow R_s^3 \frac{dR_s}{dt} = \text{constant}$$

$$R_s \approx R_s(t_{\rm rad})\,(t/t_{\rm rad})^{1/4} \quad \text{for } t \gg t_{\rm rad}$$

$$V_s \approx \frac{1}{4}\frac{R_s}{t} = \frac{1}{4} R_s(t_{\rm rad})\,(t/t_{\rm rad})^{-3/4}$$

  - This phase is called the ***momentum-conserving snowplow phase***. Towards the end of this phase, the expansion velocity becomes sonic or subsonic with respect to the interstellar sound speed.

- ***In summary, the supernova expansion velocity is continuously slowed by its interaction with the surrounding medium.***

$$R \propto t \quad \rightarrow \quad R \propto t^{2/5} \quad \rightarrow \quad R \propto t^{2/7} \quad \rightarrow \quad R \propto t^{1/4}$$

- ***Fadeaway (Merging with the ISM)***
  - For typical ISM parameters, the shock speed at the beginning of the snowplow phase is

$$V_s(t_{\rm rad}) = 188\,[{\rm km\,s^{-1}}]\,\left(E_{51}n_0^2\right)^{0.07}$$

  - This results in a very strong shock when propagating through interstellar gas with T < 10^4 K. However, the shock front gradually slows, and the shock compression declines. This proceeds until the shock speed approaches the effective sound speed in the gas and at this point the compression ratio approaches 1, and the shock wave turns into a sound wave.
  - Setting $V_s \approx c_s$ gives the a “fadeaway time”

$$V_s \approx \frac{2}{7}\frac{R_s(t_{\rm rad})}{t_{\rm rad}}\left(\frac{t}{t_{\rm rad}}\right)^{-5/7} \longrightarrow \quad t_{\rm fade} \approx \left(\frac{(2/7)R_{\rm rad}/t_{\rm rad}}{c_s}\right)^{7/5} t_{\rm rad}$$

$$t_{\rm fade} \approx 1.87\times10^6\,[{\rm yr}]\,E_{51}^{0.32}n_0^{-32}\left(\frac{c_s}{10\,{\rm km\,s^{-1}}}\right)^{-7/5}$$ end of the snowplow phase

$$R_{\rm fade} \equiv R_s(t_{\rm fade}) \approx \frac{7}{2}V_s t_{\rm fade} \approx \frac{7}{2}c_s t_{\rm fade}$$

$$\approx 2.07\times10^{20}\,[{\rm cm}]\,E_{51}^{0.32}n_0^{-0.37}\left(\frac{c_s}{10\,{\rm km\,s^{-1}}}\right)^{-2/5} \qquad 2.07\times10^{20}\,{\rm cm} = 67.1\,{\rm pc}$$

Illustration of the phases in the dynamics of a SNR

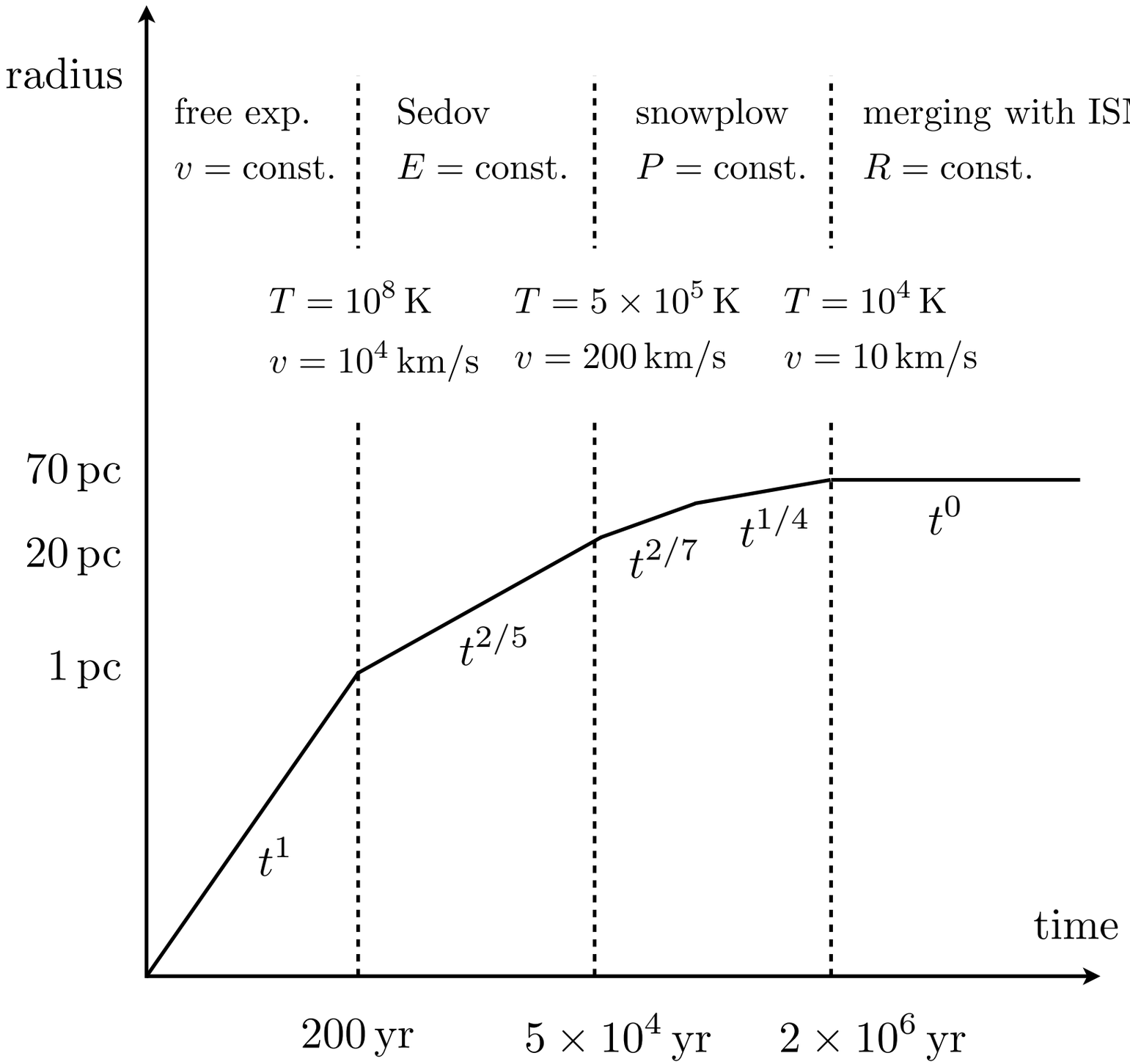

Four Phases of the SNR

1. Free Expansion Phase
2. Sedov-Taylor Phase
3. Snowplow Phase
   (pressure-driven)
   (momentum-conserving)
4. Merging Phase

Rough estimates for the temperatures and velocities at the end of each phase are given.

Fig 4.9, Rosswog & Bruggen, Introduction to High-Energy Astrophysics (slightly modified)

Morphological Types of SNRs

- SNRs have been classified into three broad categories, based primarily on their radio morphology:
  - ***Shell-like***
    - The vast majority of SNRs have the appearance of hollow “shells” with hardly any central emission (Tycho’s SNR, SNR 1006, Cassiopeia A, etc).
  - ***Crab-like*** (filled-center, Plerionic)
    - These SNRs are centrally-filled with no limb brightening. These have come to known as “plerions” (the Greek “πλήρης” meaning “full”). The Crab nebula is a prime example of this morphology.
    - The centrally-filled component in these remnants is believed to be powered by a central pulsar.
  - ***Composite*** (shell-like SNRs containing plerions)
    - This type show a shell surrounding a centrally condensed nebula. These are commonly referred to as “combination remnants”. The presence of an active pulsar at the site of the supernova explosion would naturally account for the hybrid appearance of some SNRs.
    - SNR G 326-1.8
  - ***Mixed-morphology*** (named by Jeonghee Rho)
    - Shell-like in the radio and Centrally filled in the X-ray.
    - The dominant X-ray emission is thermal despite their X-ray morphological similarity to Crab-like SNRs. The X-ray is of interstellar origin (not SN ejecta). Their formation requires a denser-than-average ISM.

SNR Examples

- Free-expansion phase
  - SN1987A, Cas A are in the free expansion phase.
  - Cassiopeia A
    - In the case of Type II supernovae resulting from core collapse in massive stars, the supernova explosion is often precede by a red supergiant phase, leaving a relatively dense circumstellar medium with a $\sim r^{-2}$ density profile.
    - The Cas A has been modeled with $M_{\rm ej} \approx 4 M_\odot$ and $E_{51} \approx 2$, expanding into a circumstellar medium with $n_{\rm H} \approx 7\,(r/{\rm pc})^{-2}\ {\rm cm}^{-3}$ left by a red supergiant phase (van Veelen et al. 2009). The reverse shock is now located at ~60% of the outer shock radius — much of Cas A ejecta is still in the free expansion phase.
    - The Cas A is at the end of its free expansion phase; it is ~ 300 years old (around 1680AD). At visible wavelengths, many ‘knots’ of emission , moving radially outward with a velocity of ~ 6000 km s^{-1}, can be seen. The knots are rich in oxygen, and are interpreted as being clumps of matter that have been ejected from the center of the star, where nucleosynthesis took place.

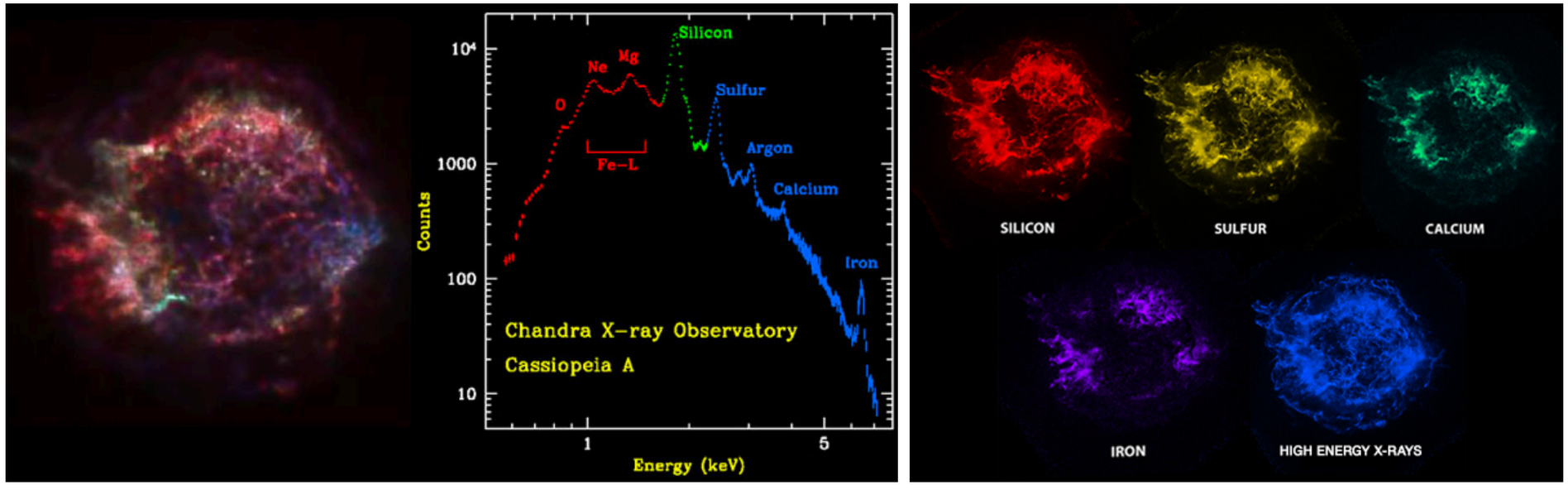

Cassiopeia A
Credit: NASA/CXC/SAO

Examples

- Sedov-Taylor phase
  - The Tycho SNR and the Crab nebular are in the Sedov-Taylor phase.
    - Light from the supernova that gave birth to the Crab Nebula was first seen on AD 1054 July 4. The SNR is at an age $t \approx 966\,\mathrm{yr}$. The solution for the Sedov-Taylor phase implies

$$R_s = A\left(\frac{E_0 t^2}{\rho_0}\right)^{1/5}, \quad V_s = \frac{dR_s}{dt} = \frac{2}{5}\frac{R_s}{t} \longrightarrow \frac{R_s}{V_s} = \frac{5}{2}t \approx 2400\,\mathrm{yr}$$

    - The azimuthally averaged radius of the Crab Nebula is $\theta \approx 150\,\mathrm{arcsec}$ in angle. The proper motion of its expansion is $\mu \approx 0.16\,\mathrm{arcsec\,yr^{-1}}$. This gives the ratio

$$\theta/\mu \approx 940\,\mathrm{yr} \longrightarrow \mu/\theta > V_s/R_s$$

      which is smaller than required by the self-similar solution.
    - This implies that V_s for the Crab Nebula is decreasing less rapidly than implied by the Sedov-Taylor solution.

Crab Nebula in multi wavelength
https://en.wikipedia.org/wiki/Crab_Nebula#/media/File:Crab_Nebula_in_Multiple_Wavelengths.png

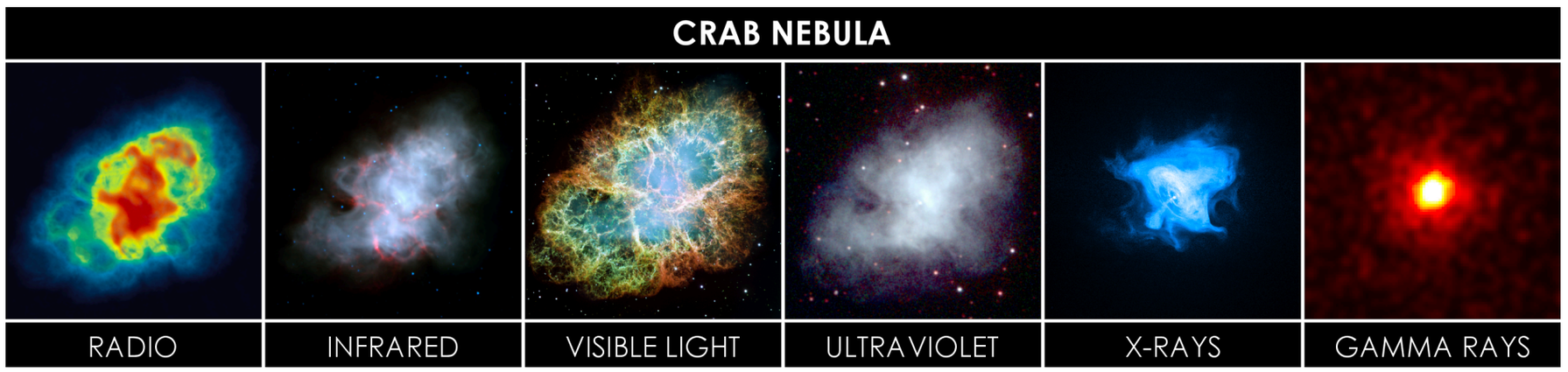

- Snowplow phase
  - Cygnus Loop
    - The Cygnus Loop (aka the Veil Nebula) is in the snowplow phase. Its age is 40,000 yr, and its expansion velocity is ~ 120 km s^{-1}. The dense shell is thermally unstable to the formation of filaments; such filaments can be seen in optically photographs of the Cygnus Loop.
    - Observationally, it is found that the internal pressure of SNRs in the snowplow phase is large enough to give a significant push to the shell.

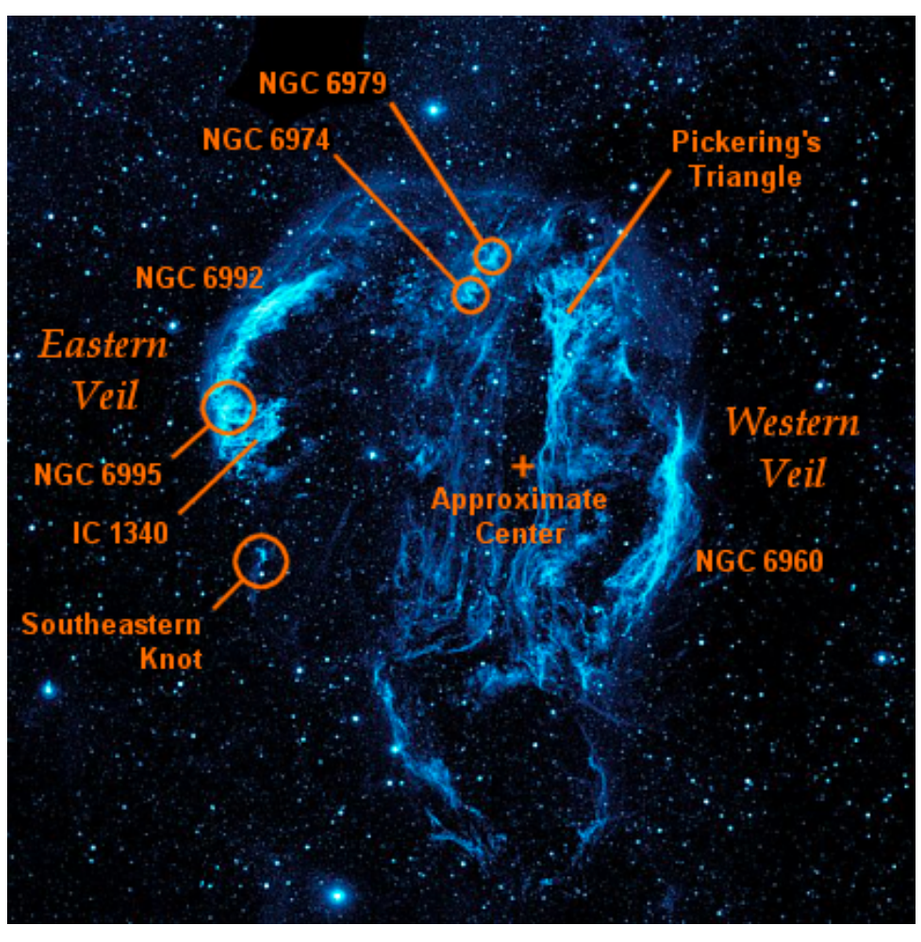

NASA/GALEX

C IV (1550Å) image
FIMS/SPEAR, STSAT-1
Seon et al. (2006, ApJL)

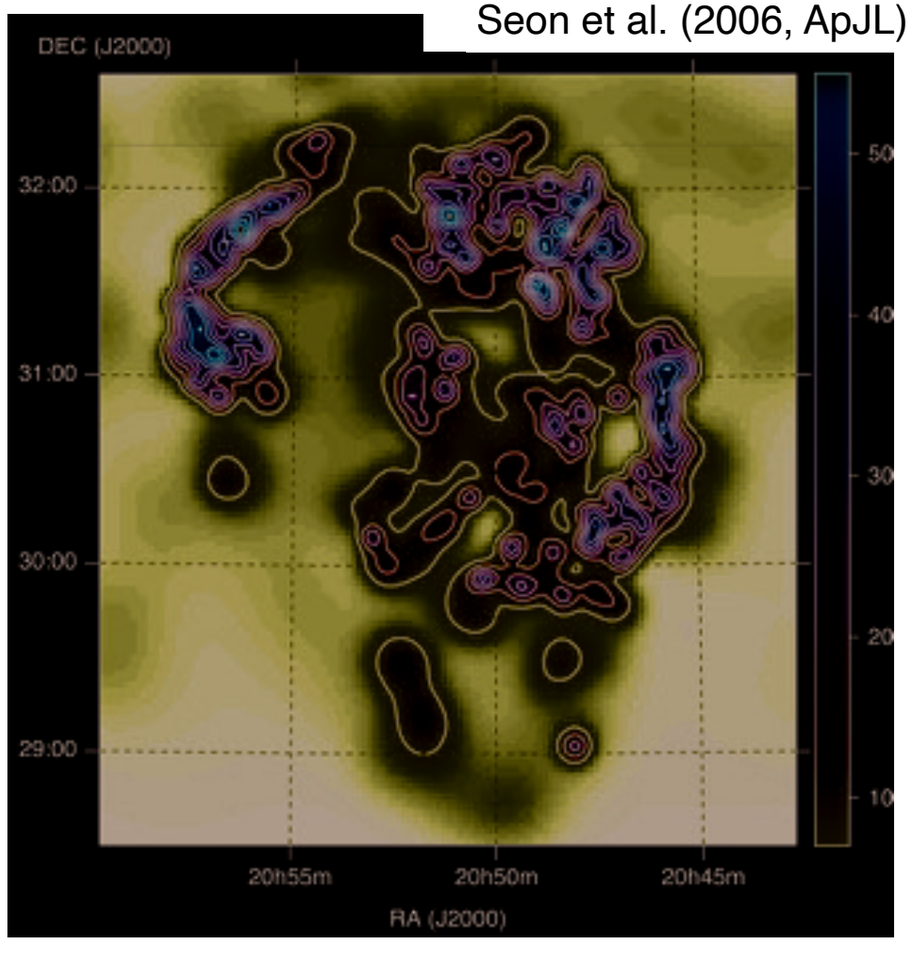

Overlapping of SNRs

- By the fadeaway time $t_{\rm fade}$, a SNR has expanded to fill a volume $(4\pi/3)R_{\rm fade}^3$
  - What is the probability that another SN will occur within this volume and affect the evolution of the original SNR before it has faded away?
  - Let a ***rate of occurrence of a SN per volume*** $S \equiv 10^{-13} S_{-13}\,{\rm pc}^{-3}\,{\rm yr}^{-1}$

    The SN rate in the Milky Way has been estimated from records of historical SNe and from observations of similar galaxies. The SN frequency in the Galaxy is estimated to be ***one event every 30-50 yr*** (Tammann et al. 1994).

    Consider the Milky Way "disk" to have a radius of 15 kpc and a thickness 200 pc, and suppose that the SN rate within this volume is 1/(60 yr). Then, this gives a SN rate per volume:

$$R = 15\,{\rm kpc} \qquad H = 200\,{\rm pc}$$

$$S = \frac{(60\,{\rm yr})^{-1}}{\pi R^2 H} \approx 1.2 \times 10^{-13}\,{\rm pc}^{-3}\,{\rm yr}^{-1} \longrightarrow S_{-13} \approx 1.2$$

- The expectation value for the number of additional SNe that will explode within this volume during the lifetime $t_{\rm fade}$ of the original SNR is

$$N_{\rm SN} = S\frac{4\pi}{3}R_{\rm fade}^3 t_{\rm fade} \approx 0.24 S_{-13} E_{51}^{1.26} n_0^{-1.47} \left(\frac{c_s}{10\,{\rm km\,s^{-1}}}\right)^{-2.6}$$

In the two-phase model of the ISM, the interstellar volume is filled by the WNM with density

$$n_0 \approx 1\,\mathrm{cm}^{-3} \text{ and } c \approx 6\,\mathrm{km\,s}^{-1}\ (T = 6000\,\mathrm{K})$$

Then, the expectation value for the number of additional SNe that will explode within this volume during the lifetime $t_{\mathrm{fade}} \approx 2\,\mathrm{Myr}$ of the original SNR is

$$N_{\mathrm{SN}} \approx 1.1$$

Therefore, we conclude that if we were to start with the two-phase model, the initially near-uniform WNM will be destroyed by the effects of SNe.

- Massive stars tend to be born in stellar associations. They enter their supernova phase before they have a chance to drift apart. Thus, the SNRs of the neighboring supernovae will merge to form a single super bubble, which may be hundreds of parsec across. Such super bubbles are a primary source of the hot ionized component of the ISM.

  In other words, SNRs will overlap and occupy a major fraction of the disk volume. This implies that, at least for the Milky Way, ***SNRs will create a multiphase ISM, consisting of low-density regions in the interior of the SNRs, and dense regions containing most of the gas mass.***

Three-Phase Model of the ISM

- An initially uniform ISM consisting of warm HI would be transformed by SNRs into a medium consisting of low-density hot gas and dense shells of cold gas.
  - This transform would take place in just a few Myr. McKee & Ostriker (1977) developed a model of the ISM that took into account the effects of these SNRs.

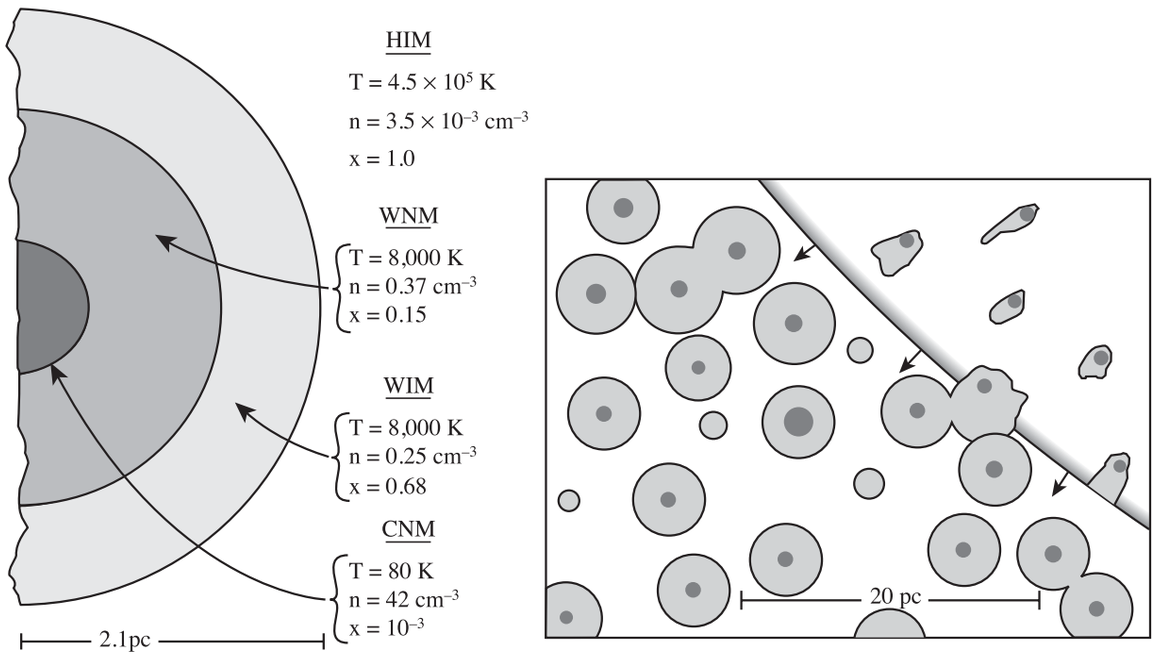

[Figure 39.3 Draine]

Left: Structure of a typical cold cloud in the three-phase model of McKee & Ostriker (1977)

Right: Close-up of a supernova blast wave.

- MO1977 argued that the pressure in the ISM was maintained by SNe.

  If initially the ISM had a low pressure, then SNRs would expand to large radii, with resulting overlap. The pressure in the ISM will rise until the SNRs tend to overlap just as they are fading, at which point the pressure in the ISM is the same as the pressure in the SNR.

- According to this argument, the overlapping condition $N_{\rm SN} \approx 1$ can be used to predict the pressure of the ISM.

- We can express the expectation value for overlap in terms of the pressure:

$$N_{\rm SN} \approx 0.24 S_{-13} E_{51}^{1.26} n_0^{-1.47} \left(\frac{c_s}{10\,{\rm km\,s^{-1}}} \right)^{-2.6}$$

We can eliminate the sound speed in favor of the pressure:

$$P = 1.4\, n_{\rm H} m_{\rm H} c_s^2$$

$$\longrightarrow \quad N_{\rm SN} \approx 0.48 S_{-13} E_{51}^{1.26} n_0^{-1.47} \left(\frac{P/k}{10^4\,{\rm cm^{-3}\,K}} \right)^{-1.3}$$

We can solve for the pressure

$$P/k = 5700\,[{\rm cm^{-3}\,K}]\, S_{-13}^{0.77} E_{51}^{0.97} n_0^{-0.13} N_{\rm SN}^{-0.77}$$

$$P/k \approx 6600\,{\rm cm^{-3}\,K} \text{ for } S_{-13} \approx 1.2$$

This is comparable to the observed thermal pressure $P/k \approx 3800\,{\rm cm^{-3}\,K}$ in the ISM today.

- ***The principal shortcoming of the MO77 three-phase model is the failure to predict the substantial amount of the warm HI gas.*** The model predicts only 4.3% of the HI mass in the warm phase (WNM and WIM). The 21-cm line observations indicate that more than 60% of the HI within 500 pc of the Sun is actually in the warm phase (Heiles & Troland 2003).

Observing the HIM - Local Bubble

- How to observe the HIM - Emission Lines?
  - HII regions have readily observable emission lines that let us estimate their density and temperature.
  - However, finding the density and temperature of the HIM is more difficult.
  - The temperature of the HIM, T ~ 10^6 K, corresponds to $h\nu \sim kT \sim 100\,\mathrm{eV}$. However, photons with an energy 100 eV (~ 120Å) are difficult to observe, even if we use space observatories.
    - This is primarily because of the large photoionization cross-section of hydrogen.

$$\sigma_{\mathrm{pi}} \approx 6.3 \times 10^{-18}\,\mathrm{cm}^2\ (h\nu/I_{\mathrm{H}})^{-3}$$

    - A column depth N(HI) > 10^{20} cm^{-2} (corresponding to ~ 20 pc through the WNM, ~ 1 pc through the CNM) will absorb nearly all 100 eV photon that is emitted by a bubble of hot gas.

- The only portion of the HIM from which we can observe 100 eV photon is the Local Bubble.

- Soft-Xray (1/4 keV) background, the Local Hot Bubble

hard-xray: E > 1 keV

  - The X-ray background is an unexpectedly intense diffuse flux of soft X-rays (Bowyer et al. 1968). X-ray at the low energies are easily absorbed by interstellar clouds, so it was concluded that they must have a local origin. Moreover, observations show that there is a suspicious lack of cool, absorbing gas with about ~ 100 pc of the Sun.
  - The existence of the local hot bubble has been proposed to explain the soft X-ray background. The local bubble is a cavity in the ISM filled with hot, X-ray-emitting gas.
  - A nearby supernova explosion could carve the bubble out millions of years ago, leaving a region filled with relatively little neutral hydrogen, but a lot of 10^6 K gas.
  - But this paradigm was challenged when X-rays emanating from a comet as it passed through the solar wind.
  - When the charged ions flowing out from the Sun collide with neutral hydrogen and helium atoms in interplanetary space, they can exchange electrons, producing soft X-ray photons in the process. If the X-ray emission caused by the solar wind could account for the entire X-ray background, then it would negate the need for a local hot bubble.
  - Galeazzi et al. (2014, Nature) combined observations from the “Diffuse X-rays from the Local galaxy” (DXL) rocket mission with the ROSAT data and found that ***the X-ray emission from solar wind could only account for about 40% of the diffuse X-ray background.***

The Local Bubble (NASA CHIPS)

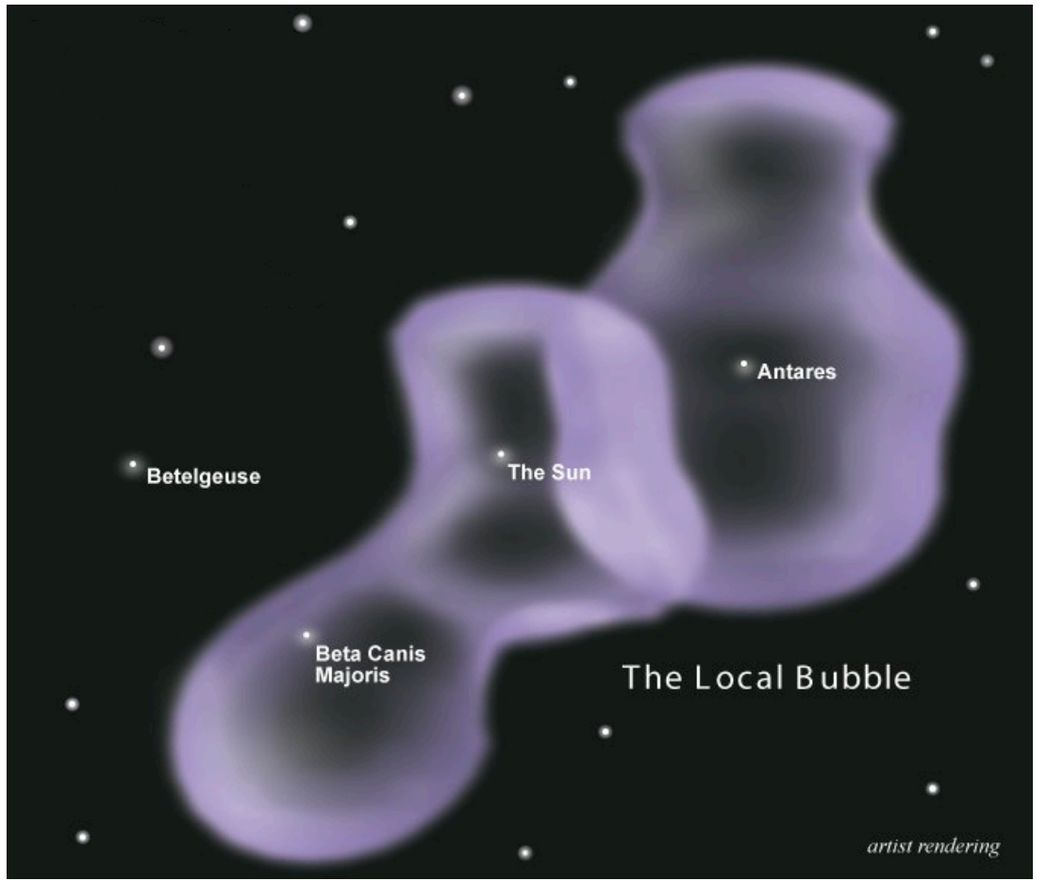

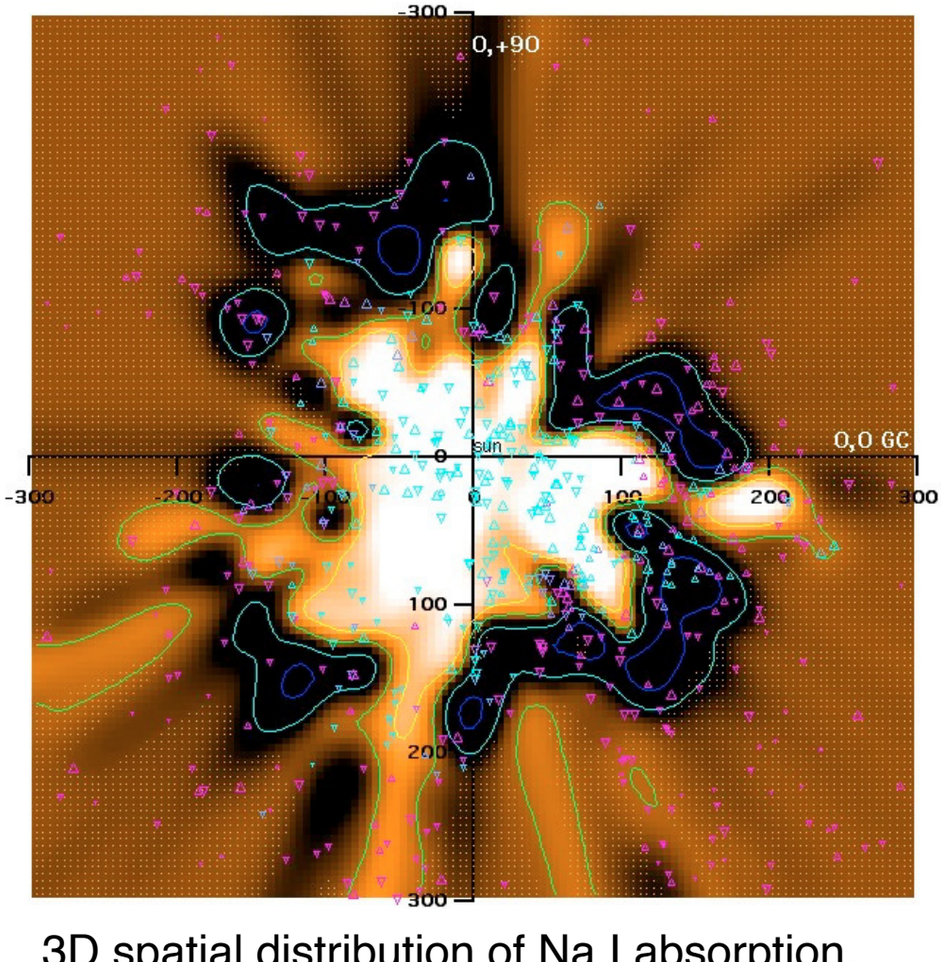

3D spatial distribution of Na I absorption, as viewed in the Galactic plane projection. (Welsh et al. 2010)

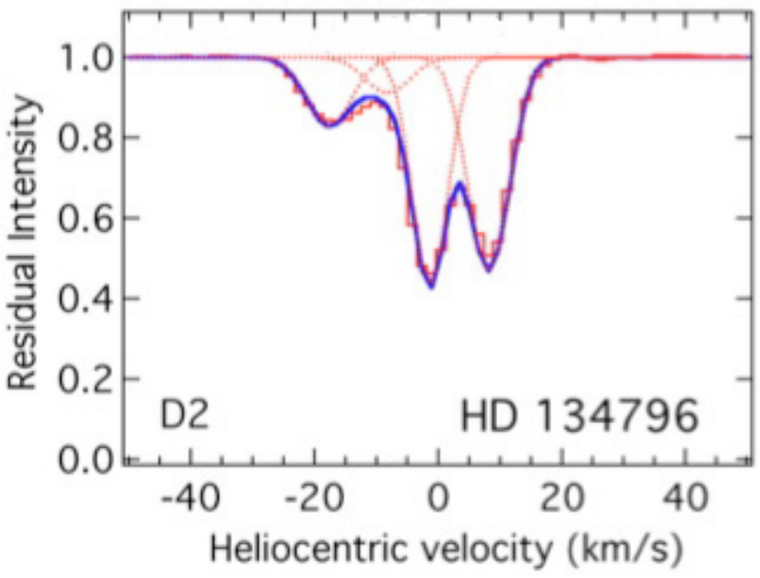

An example spectrum of Na I absorption line (Welsh et al. 2010)

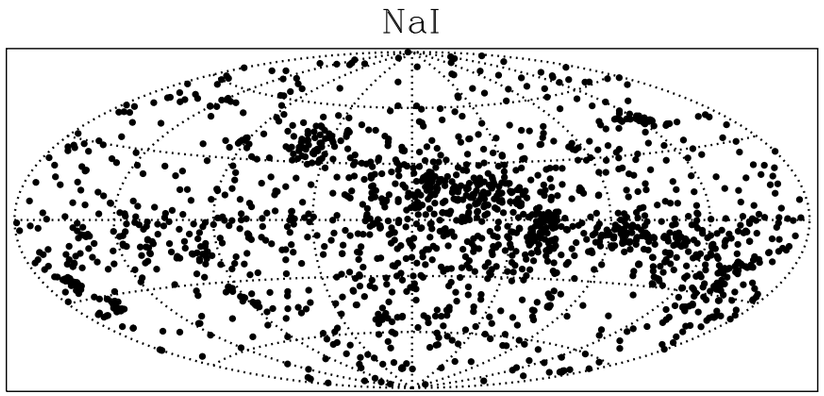

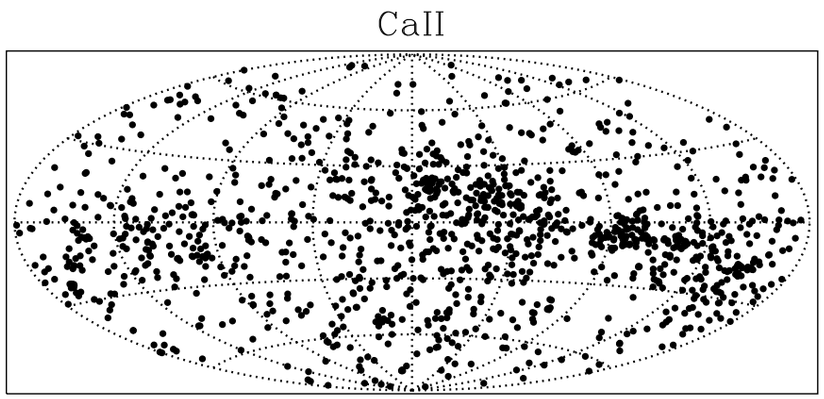

Sightlines for Na I and Ca II absorption line observations (Welsh et al. 2010)

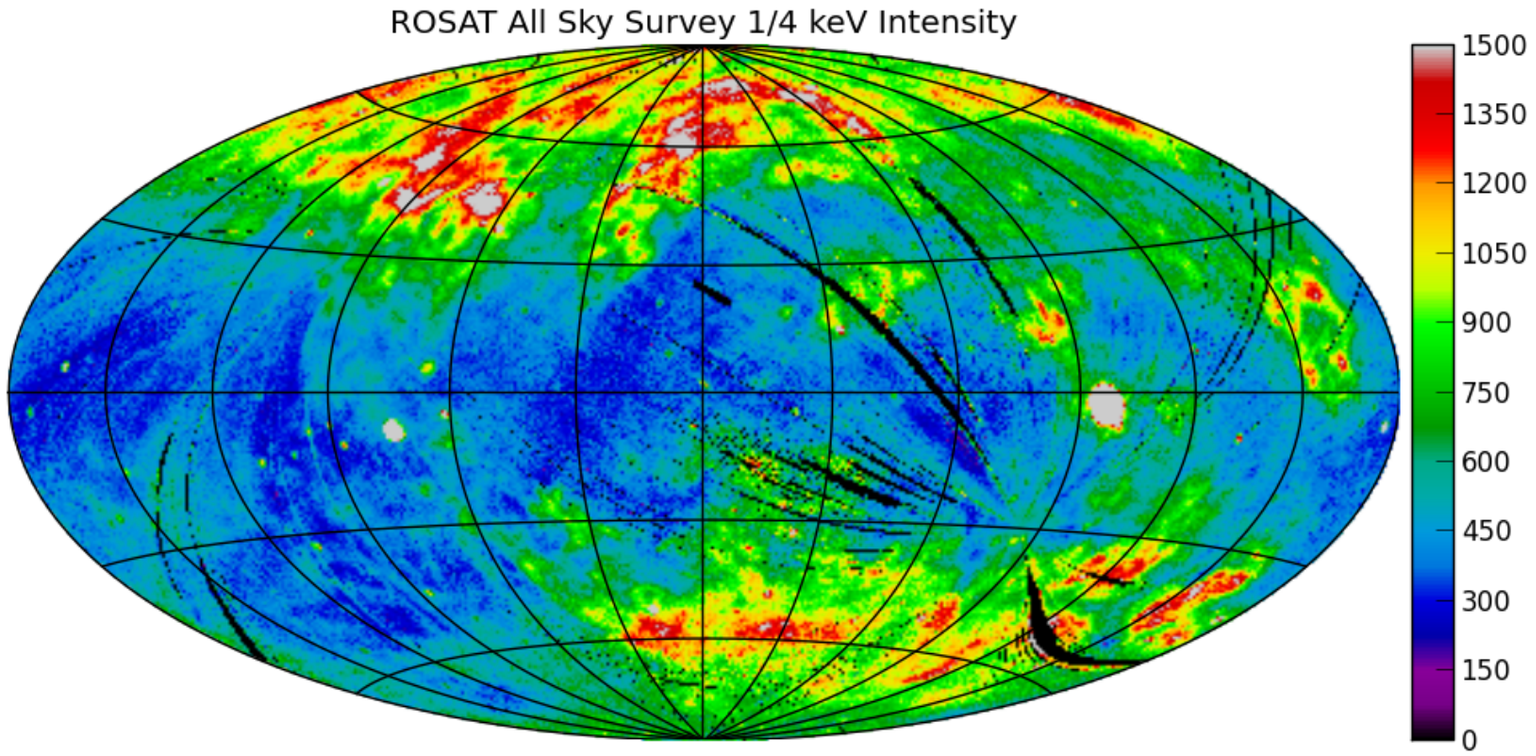

intensity unit = 10^{-6} counts s^{-1} $arcmin^{-2}$ (Slavin, 2017)

- Emission Lines from the Local Bubble?
  - At T ~ 10^6 K, hydrogen and helium is fully ionized. The most abundant heavy elements (oxygen, carbon, and neon) are primarily helium-like. The dominant forms of iron are Fe IX, X, and XI.
  - The iron ions from Fe IX to Fe XI produce a cluster of emission lines near (λ ~ 180Å). About half of the radiated power come out in the form of these iron emission lines.
  - Iron isn't fully ionized until T > 2x10^8 K. At T ~ 10^7 K, the dominant forms are Fe XX and XXI.

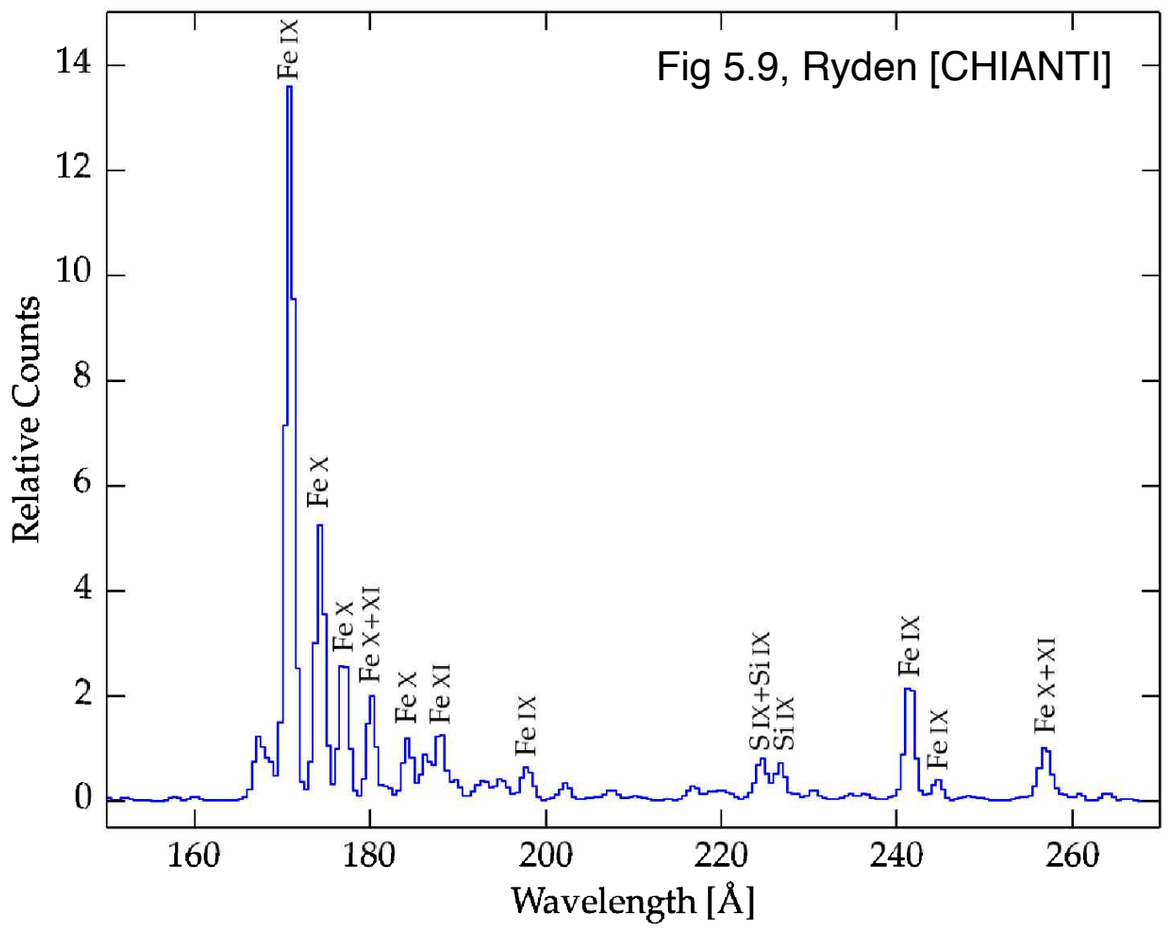

  - However, observations at λ ~ 180Å by the Cosmic Hot Interstellar Plasma Spectrometer (CHIPS) showed that the Fe emission lines from the Local Bubble are much weaker than originally predicted.
  - This might be attributable to (1) depletion of iron onto dust grains, (2) a somewhat lower temperature (7x10^5 K), and (3) delayed recombination.
  - The Local Bubble is still being cooling, and Fe is more highly ionized than CIE tells us.

- Absorption Lines from the Local Bubble.
  - One important pair of UV lines is the Lithium-like OVI doublet 1032Å (12.01 eV) and 1038Å (11.95 eV). These lines are a major coolant for interstellar gas at T ~ $3x10^5$ K.
  - At T ~ $3x10^5$ K, only ~ 25% of the total oxygen abundance is O VI (~35% is OV and ~35% is OVII). However, the O VI doublet lines have a large cross section, and thus are readily observed even if the number density of OVI ions is small.
  - To detect the OVI lines in absorption, we need background sources with $T_{eff} > 1.4x10^5$ K (12 eV). Main sequence stars are not this hot. So, we have to look at nearby, young, hot white dwarfs. In particular, white dwarfs of spectral type DA, which have only hydrogen lines in their spectra, are the best targets.

- The distribution of OVI in the Local Bubble appears to be patchy, and the mean density of OVI lies in the range N(OVI)/d ~ (0.7 - 13)$x10^{-8}$ cm^{-3}. (See Savage & Lehner 2006).
- The thermal broadening parameter was found to range from b = 15 km s^{-1} to 36 km s^{-1}. From this, we can find a temperature:

$$T = 2.5 \times 10^5 \,\mathrm{K} \left(\frac{b}{16 \,\mathrm{km\,s^{-1}}} \right)^2 \left(\frac{m}{16\, m_\mathrm{H}} \right)$$

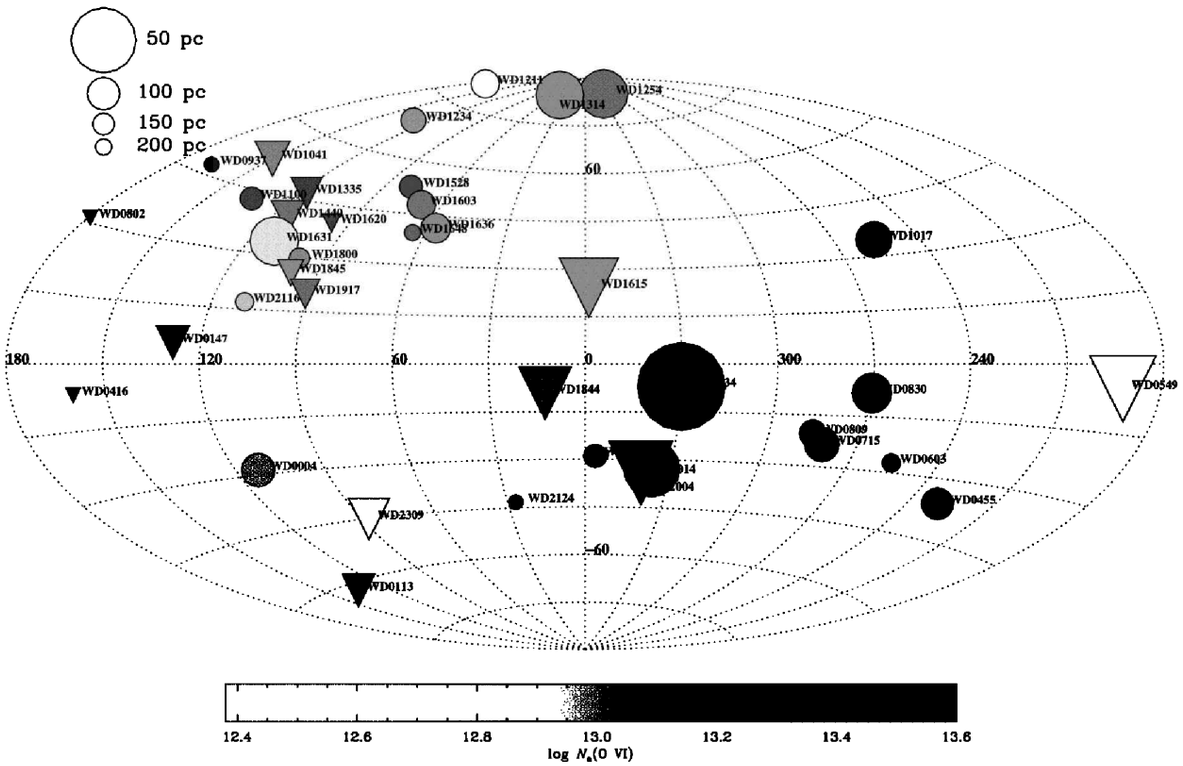

$N(\mathrm{O\,VI}) \approx 10^{13} - 10^{13.6}\,\mathrm{cm}^{-2}$

Location in galactic coordinates of 39 nearby hot DA white dwarfs (Savage & Lehner 2006).

Circles have OVI detection; triangles are non-detections at 2σ level.
Grayscale indicates the column density of OVI toward white dwarfs with detections.

Fig 5.11 [Ryden]

FUV Emission Line Maps of the Milky Way (FIMS/SPEAR, STSAT-1)

C IV 1548, 1551Å

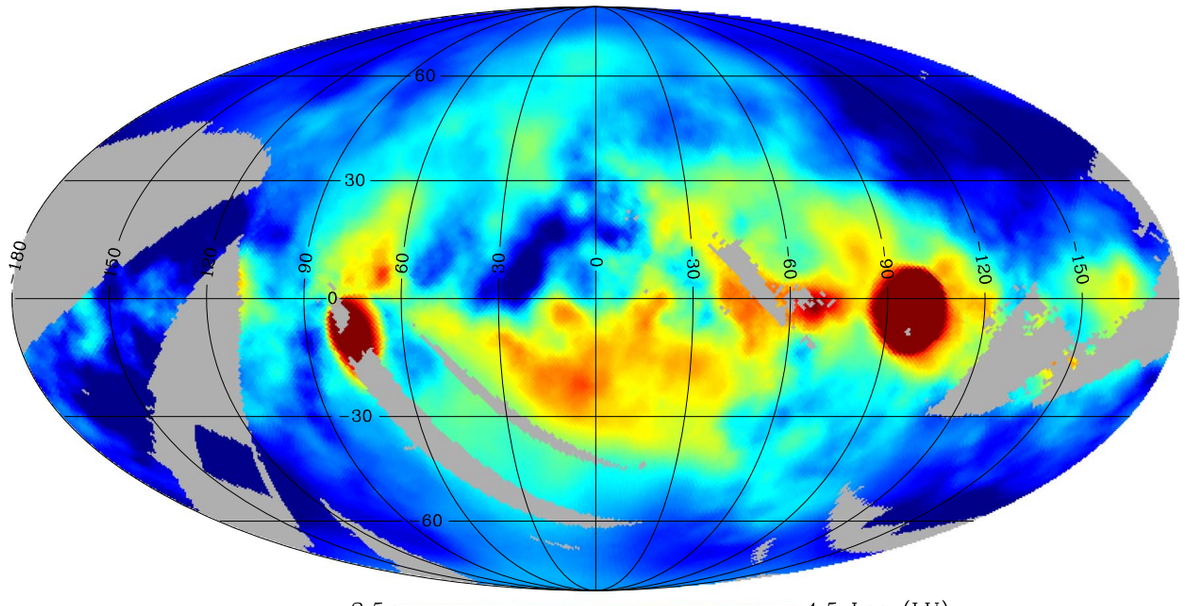

O VI 1032, 1038Å

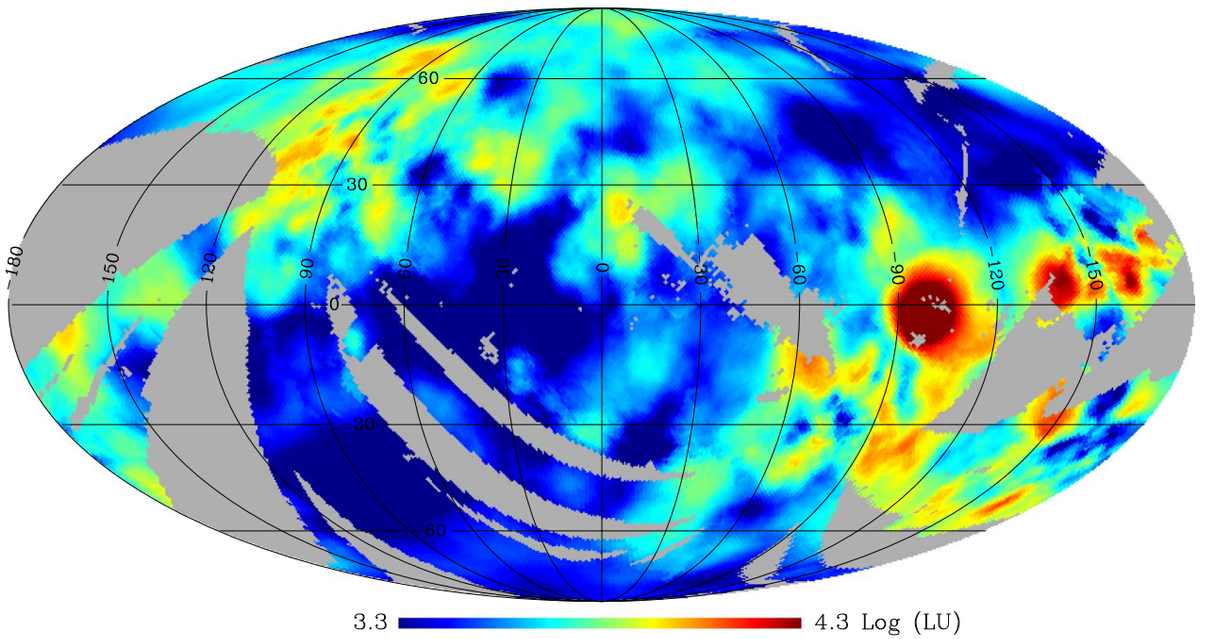

LU (Line Unit) = photons cm^{-2} s^{-1} sr^{-1}
Jo, Seon, et al. (2019, ApJS)

Dust

- Observed Properties
- Dust Materials

Observed Properties

- Observational Evidence on the presence of dust grains in the ISM
  - Wavelength-dependent attenuation (“extinction”) of starlight by absorption and scattering, observable in a wavelength range of 20μm to 0.1 μm. The extinction includes a number of spectral features that provide clues to grain composition.
  - Wavelength-dependent polarization of starlight
  - Scattered light in reflection nebulae
  - Thermal emission from dust, at wavelengths ranging from the sub-mm to 2μm.
  - Small-angle scattering of X-rays, resulting in “scattering halos” around X-ray point sources.
  - Microwave emission from dust, probably from rapidly spinning ultra-small grains.
  - Luminescence when dust is illuminated by starlight — the so-called extended red emission.

- Extinction = Absorption + Scattering
  - Dust particles can scatter light, changing its direction of motion. When we look at a reflection nebula, like that surrounding the Pleiades, we are seeing light from the central stars that has been scattered by dust into our line of sight.
  - Dust particles can also absorb light. The relative amount of scattering and absorbing depends on the properties of the dust grains.
  - When we look at a distant star through the intervening dust, the excess dimming of the star is caused by a combination of scattering and absorbing as extinction.
- Thermal radiation from Dust
  - When dust absorbs light, it becomes warmer, so dust grains can emit light in the form of thermal radiation. Most of this emission is at wavelengths from a few microns (near IR) to the sub-mm range (Far-IR).
- Polarization
  - The polarization of starlight was discovered in 1949 (Hall 1949).
  - The degree of polarization tends to be larger for stars with greater reddening, and stars in a given region of the sky tends to have similar polarization directions.

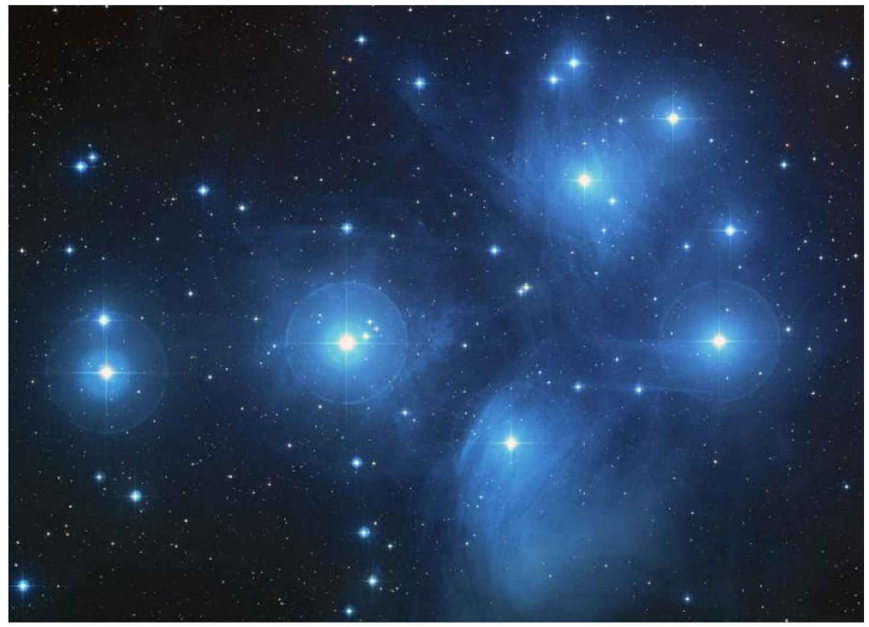

The Pleiades cluster and surrounding reflection nebulae (Fig. 6.3, Ryden)

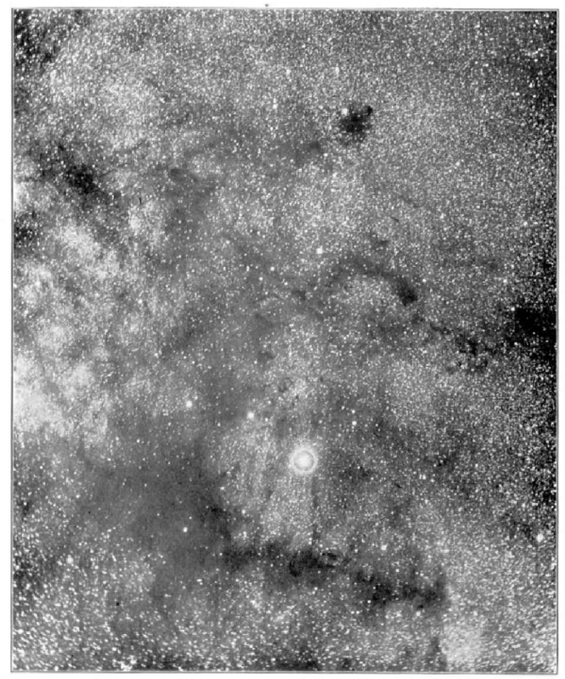

The dark structures near θ Ophiuchi (Barnar 1899; Fig. 6.1, Ryden)

Dust matters!

- Importance of Dust
  - In our Galaxy, the gas-to-dust ratio is about 100:1 by mass. Since the ISM is about 10% of the baryonic mass of the Galaxy, dust grains comprise roughly 0.1% of the total baryonic mass.
  - Dust grains absorb roughly 30-50% of the starlight emitted by the Galaxy and re-emit it as far-infrared continuum emission. ***This means that only 0.1% of the baryons are ultimately responsible for a third to a half of the bolometric luminosity of the Galaxy.***
  - Dust grains are the central to the chemistry of interstellar gas. ***The abundance of H_2 in the ISM can only be understood if catalysis on dust grains is the dominant formation avenue.***
  - The formation of planetary system is believed to begin when dust grains in a protostellar disk begin to coagulate into larger grains, leading to planetesimals and eventually to planets, carrying their complex organic molecules with them.

Interstellar Extinction

- History - extinction
  - Barnard (1907, 1910) was apparently the first to realize that some stars were dimmed by an “absorbing medium.”
  - Trumpler (1930) showed that the stars in distant open clusters were dimmed by something in addition to the inverse square law, and concluded that interstellar space in the galactic plane contained “fine cosmic dust particles of various sizes… producing the observed selective absorption.”
- Pair method
  - Trumpler compared the spectra of pairs of stars with identical (or similar) spectral type, one with negligible obscuration and the other extinguished by dust along the line of sight. This method remains our most direct way to study the “selective extinction” or “reddening” of starlight by the interstellar dust.

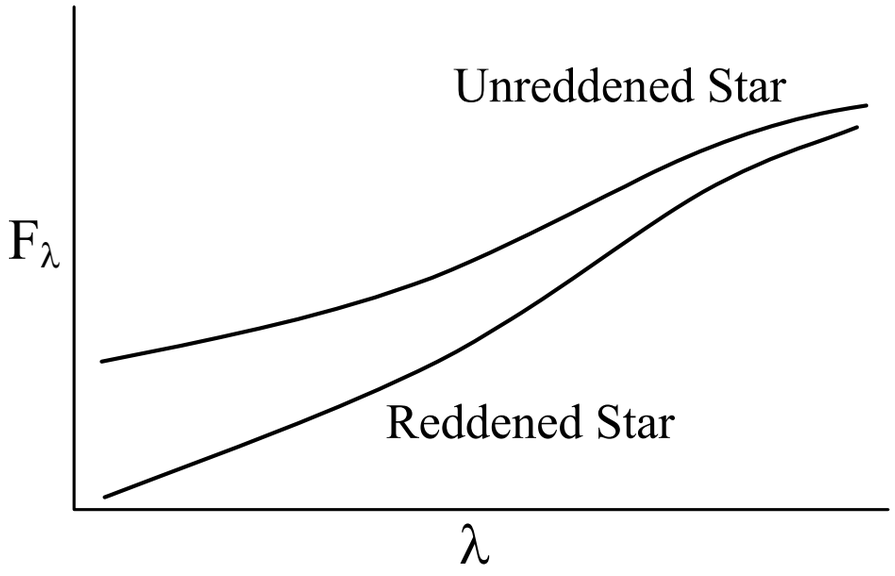

- Because atomic hydrogen absorbs strongly for $h\nu > 13.6\,\mathrm{eV}$, it is possible to measure the contribution of dust to the attenuation of light only at $h\nu < 13.6\,\mathrm{eV}$ or λ > 912 Å.

- ***Extinction***
  - Astronomers characterize the attenuating effects of dust by the "extinction" A_λ at wavelength λ. The extinction at a particular wavelength λ, measured in "magnitudes" is defined by the difference between the observed magnitude m_λ and the unabsorbed magnitude m_λ^0:

$$\begin{aligned} A_\lambda\ [\mathrm{mag}] &= m_\lambda - m_\lambda^0 \\ &= -2.5 \log_{10} \left(\frac{F_\lambda}{F_\lambda^0} \right) \end{aligned}$$

F_λ = the observed flux from the star

F_λ^0 = the flux that would have been observed if the only attenuation had been from the inverse square law.

$$F_\lambda = F_\lambda^0 e^{-\tau_\lambda}$$

- The extinction measured in magnitudes is proportional to the optical depth:

$$\begin{aligned} A_\lambda &= 2.5 \log_{10} \left(e^{\tau_\lambda} \right) = 2.5 \log \left(e \right) \times \tau_\lambda \\ &= 1.086 \tau_\lambda \end{aligned}$$

- ***The Reddening Law, Extinction Curve***
  - Extinction curve - the extinction A_λ as a function of wavelength or frequency
    - A typical extinction curve shows the ***rapid rise in extinction in the UV***.
    - ***The extinction increases from red to blue***, and thus the light reaching us from stars will be "reddened" owing to greater attenuation of the blue light.
    - The reddening by dust is expressed in terms of a color excess; for instance, $\lambda_B \sim 4400\,\text{Å}$ $\lambda_V \sim 5500\,\text{Å}$

B-V color: $m_B - m_V$

B-V color excess: $E(B-V) \equiv (m_B - m_V) - (m_B^0 - m_V^0) = A_B - A_V$

in general, $E(\lambda_1 - \lambda_2) \equiv A_{\lambda_1} - A_{\lambda_2} \quad (\lambda_1 < \lambda_2)$

- The detailed wavelength dependence of the extinction - the "reddening law" - is sensitive to the composition and size distribution of the dust particles.
- The slope of the extinction at visible wavelengths is characterized by the dimensionless ratio, the ratio of total to selective extinction:

$$R_V \equiv \frac{A_V}{A_B - A_V} \equiv \frac{A_V}{E(B-V)}$$

- R_V ranges between 2 and 6 for different lines of sight. Sightlines through diffuse gas in the Milky Way have $R_V \approx 3.1$ as an average value. ***Sightlines through dense regions tend to have larger values of*** R_V***.*** In dense clouds, the value $R_V \approx 5$ is typically adopted.

- ***Observed extinction curves vary in shape from one line of sight to another.***
- Extinction curve, relative to the extinction in the Cousins I band (λ = 8020Å), as a function of inverse wavelength, for Milky Way regions characterized by different values of R_V.

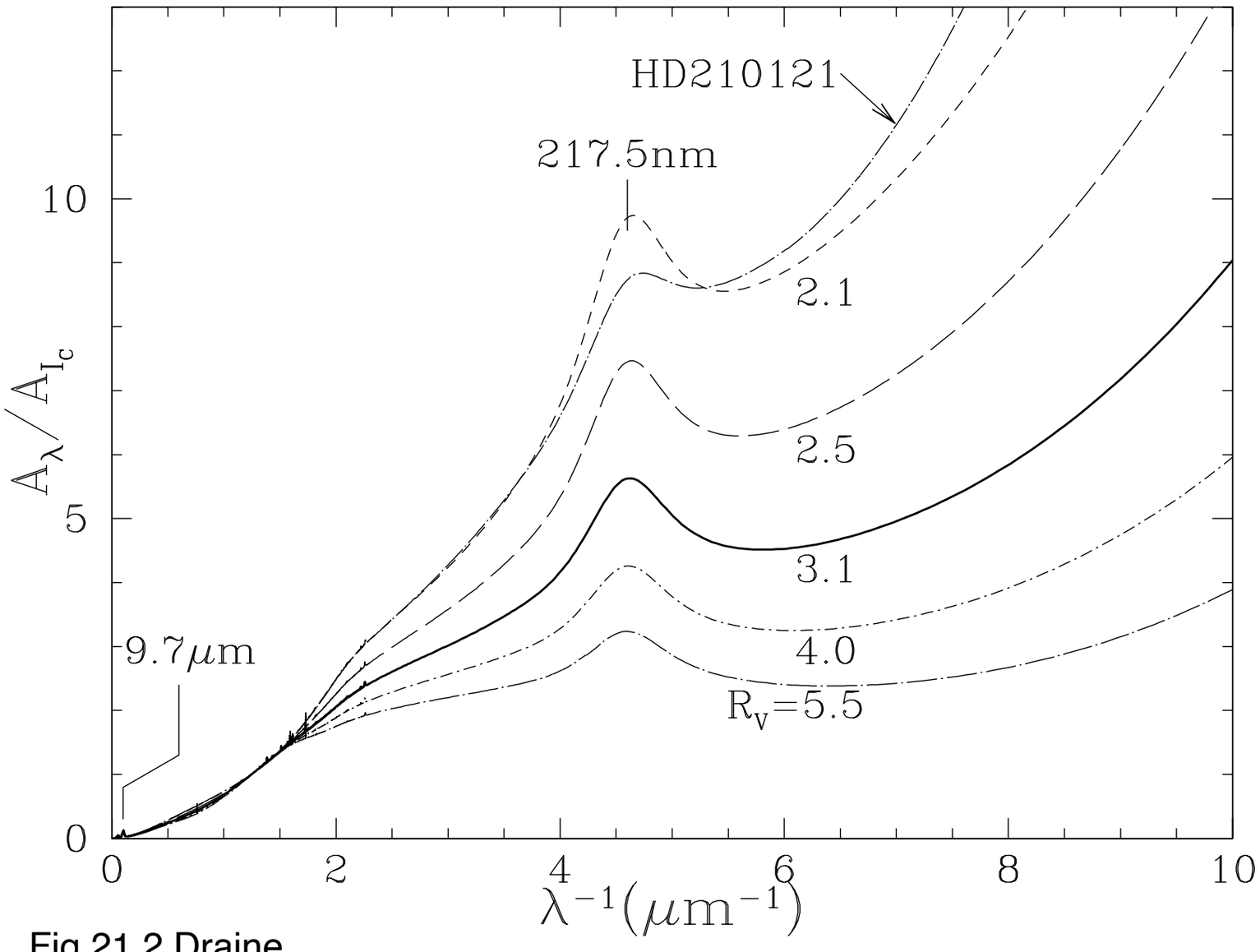

Fig 21.2 Draine

Cardelli et al. (1989) showed that the optical-UV extinction can be approximated by ***a one-parameter family of curves***, parameterized by R_V,

$$A_\lambda / A_{\lambda_{\rm ref}} \approx f_1^{\rm CCM}(\lambda;\, R_V)$$

Fitzpatrick (1999) recommends a slightly modified function, which has been used to generate the synthetic extinction curves shown in the left side.

The extinction model was extended into the infrared by Draine (1989).

Note that the extinction curve toward the star HD210121 (with R_V = 2.1) differs from the CCM extinction curve for R_V = 2.1.

- If the dust grains were large compared to the wavelength, we would be in the "geometric optics" limit, and the extinction cross section would be independent of wavelength (gray extinction), with $R_V = \infty$.
  - The tendency of the extinction to rise with decreasing λ, even at the shortest ultraviolet wavelengths tells us that grains smaller than the wavelength must be making an appreciable contribution to the extinction at all observed wavelengths, down to λ = 0.1μm.
  - As we will see later, "small" means (approximately) that $2\pi a/\lambda \lesssim 1$. Thus interstellar dust must include a large population of small grains with $a \lesssim 0.015\,\mu\mathrm{m}$.
- The dust appears to be relatively well-mixed with the gas (Bohlin et al. 1978; Rachford et al. 2009):

$$\frac{N_{\mathrm{H}}}{E(B-V)} = 5.8 \times 10^{21}\,\mathrm{H\,cm^{-2}\,mag^{-1}}$$

$N_{\mathrm{H}} \equiv N(\mathrm{HI}) + 2N(\mathrm{H_2})$

column density of total hydrogen nuclei

  - For sightlines with $R_V \approx 3.1$, this implies that

$$\frac{A_V}{N_{\mathrm{H}}} \approx 5.3 \times 10^{-22}\,\mathrm{mag\,cm^2\,H^{-1}}$$

  - Thus, even at high galactic latitudes, where the column density of hydrogen is ~ 10^{20} cm^{-2}, there is still some foreground extinction when looking at extragalactic sources; ~ 0.05 magnitudes in the V band.

- ***Scattering of Starlight***
  - When an interstellar cloud happens to be unusually near one or more bright stars, we have a reflection nebula, where we see starlight photons that have been scattered by the dust in the cloud.
  - ***The spectrum of the light coming from from the cloud surface shows the stellar absorption lines***, thus demonstrating that scattering rather than some emission process is responsible.

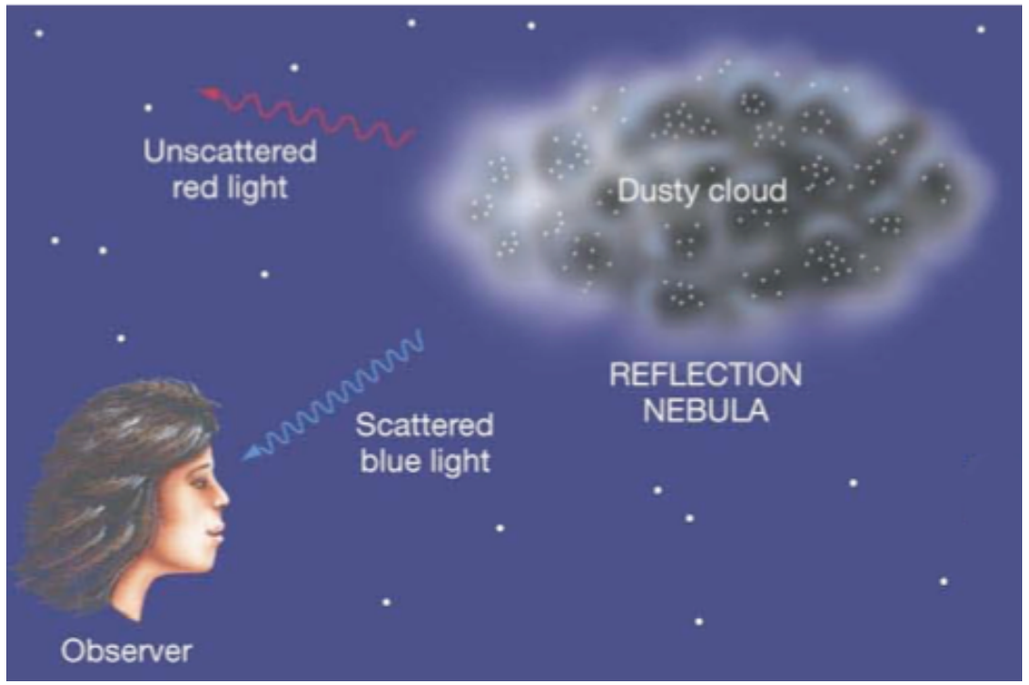

  - Given the typical size of interstellar dust grains, blue light is scattered more than red light. ***A reflection nebulae is typically blue*** (so for the same reason that the sky is blue, except it's scattering by dust (for the reflection nebula) vs by molecules (for the earth's atmosphere)).
  - By comparing the observed scattered intensity with the estimated intensity of the starlight incident on the cloud, it is possible to infer the albedo of the dust - the ratio of scattering cross section to extinction cross section.

Diffuse Galactic Light (DGL)

- The term DGL denotes the diffuse component of the galactic background radiation which is produced by scattering of stellar photons by dust grains in interstellar space.
- The DGL is most intense in directions where the dust column density and the integrated stellar emissivity are both high.

- The study of dust scattering properties has shed light on the nature of the 2175Å bump and the far-ultraviolet rise features of extinction curves.
- Lillie & Witt (1976) and Calzetti et al. (1995) showed that the 2175Å bump was likely an absorption feature with no scattered component.
- The current data indicates the wavelength dependence of the albedo is ~ 0.6 in the NIR/ optical with a dip to ~ 0.4 for 2175Å bump, a rise to ~ 0.8 around 1500Å, and a drop to ~0.3 by 1000Å.

The determinations of the albedo in reflection nebulae, dark clouds, and the DGL are plotted versus wavelength.

Predictions from dust grain models are also plotted for comparison.

Karl D. Gordon,
2004, ASPC, 309, 77

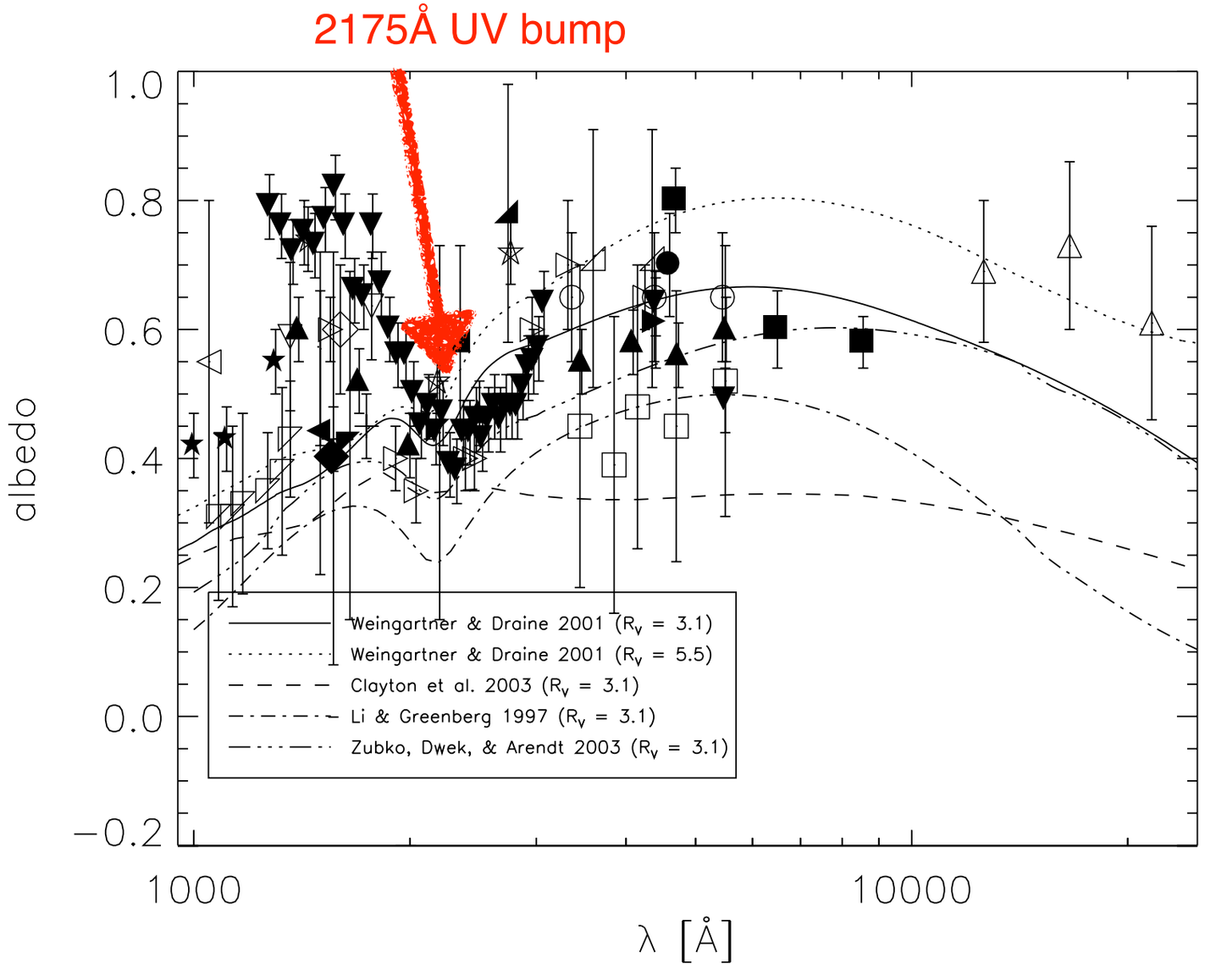

- ***Polarization of Starlight by Interstellar Dust***
  - Initially unpolarized light propagating through the ISM becomes linearly polarized as a result of preferential extinction of one linear polarization mode relative to the other.

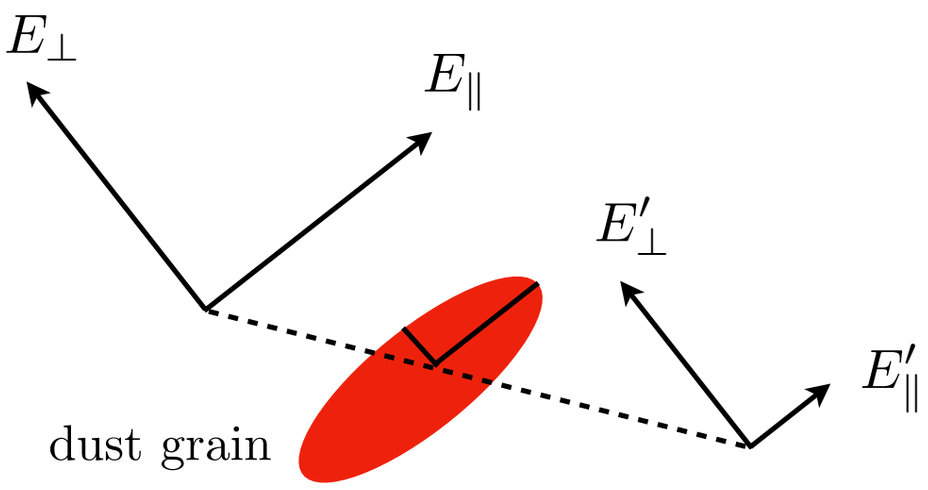

$$E_\parallel = E_\perp \qquad E'_\parallel = E_\parallel e^{-\tau_\parallel}$$
$$E'_\parallel < E'_\perp \qquad E'_\perp = E_\perp e^{-\tau_\perp}$$
$$\tau_\parallel > \tau_\perp$$

The starlight is slightly more blocked along the long axis of the grains than along the short axis. This give rise to the polarization of starlight.

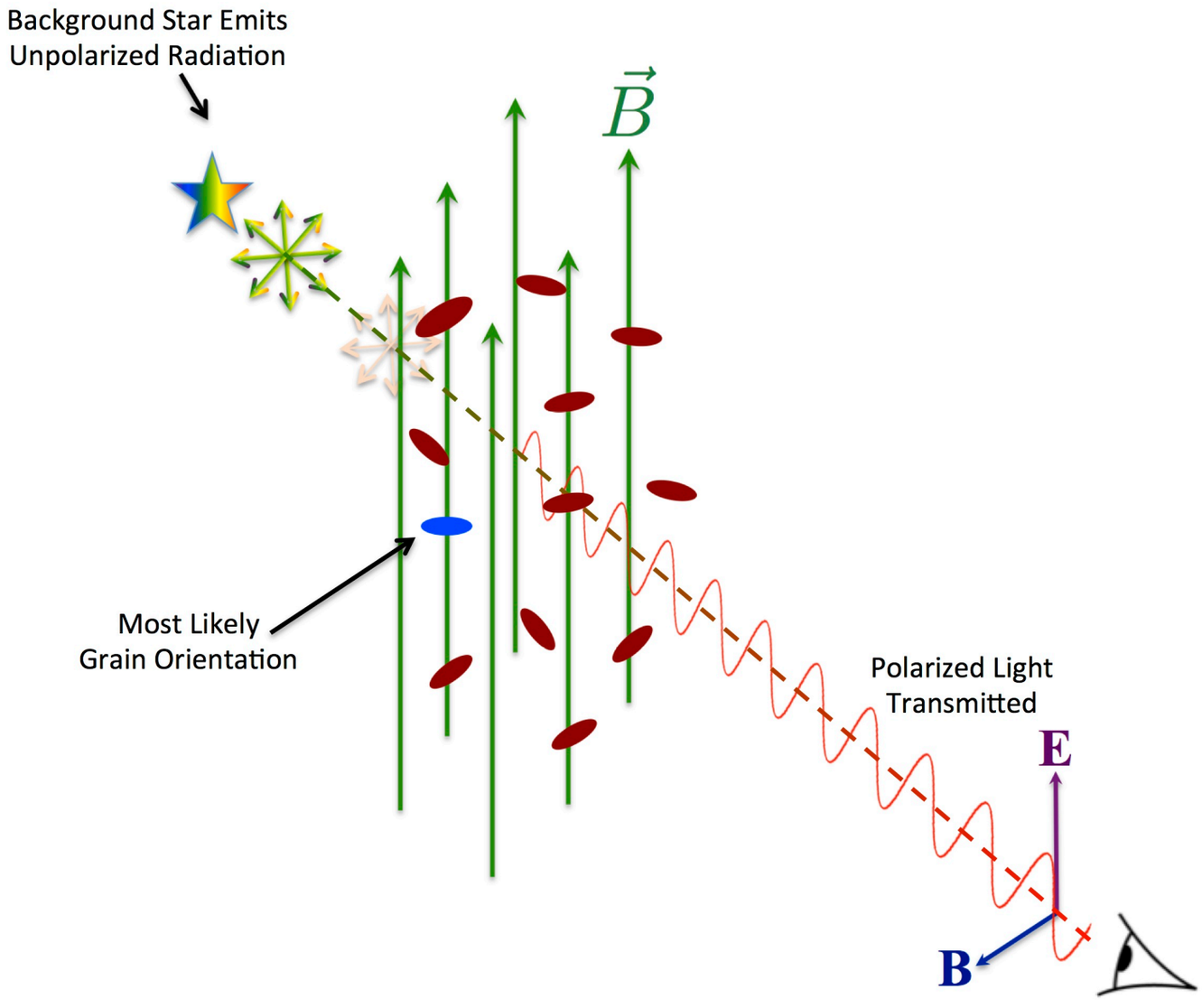

credit: B-G Andersson

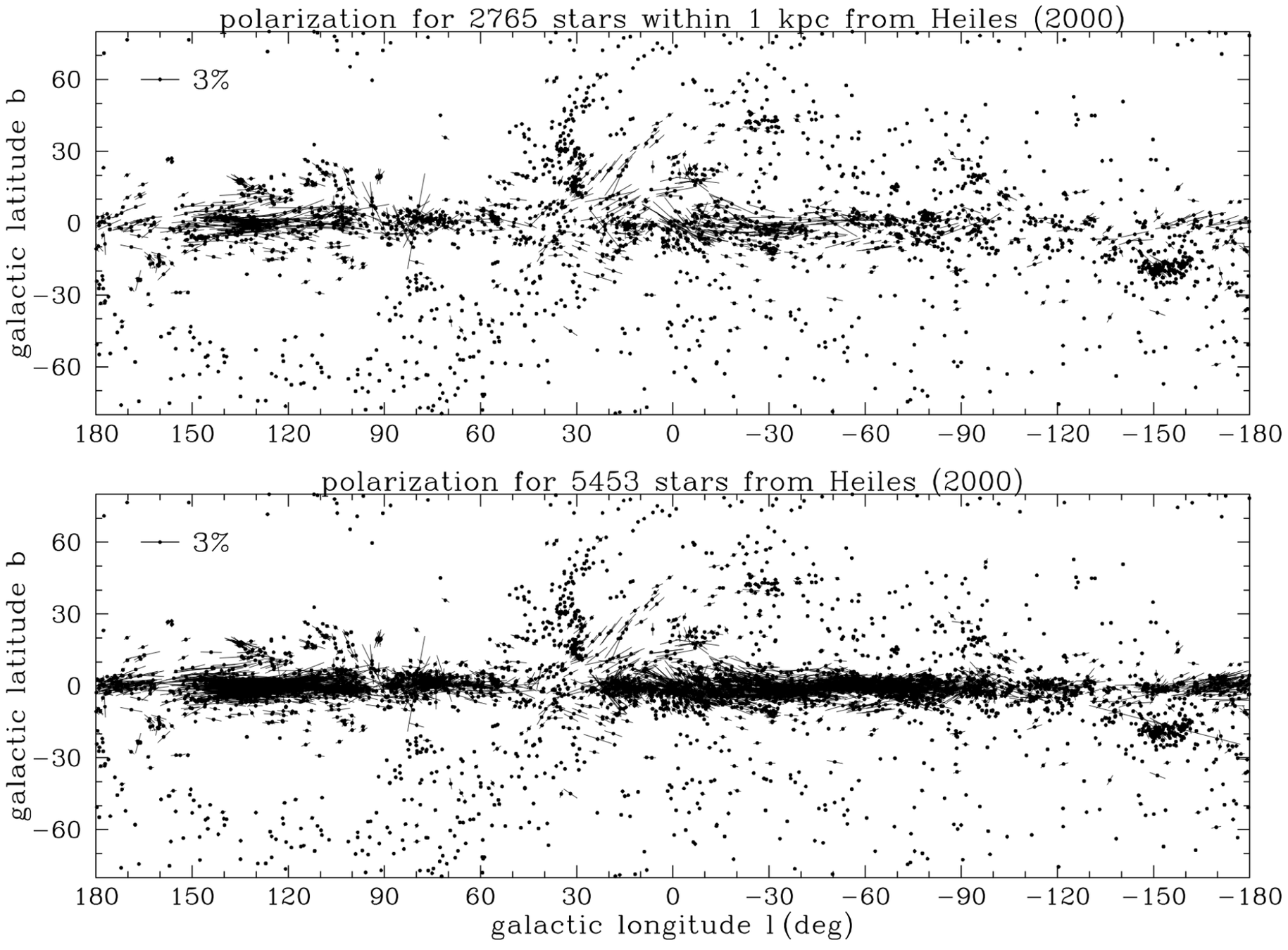

[Fig 21.3, Draine; Heiles (2000)]

- The polarization percentage typically peaks near the V band (5500Å), and can be empirically described by the ***"Serkowski law"*** (Serkowski 1973):

$$p(\lambda) \approx p(\lambda_{\max}) \exp\left[-K \ln^2(\lambda/\lambda_{\max})\right]$$

$\lambda_{\max}$ = the wavelength of the maximum polarization

$$K = 1.86(\lambda_{\max}/\mu\mathrm{m}) - 0.1$$

$$\lambda(\mu\mathrm{m}) \approx (0.17 \pm 0.05) R_V$$
$$0.34\mu\mathrm{m} \lesssim \lambda_{\max} \lesssim 1\mu\mathrm{m}, \quad \langle\lambda_{\max}\rangle \approx 0.55\mu\mathrm{m}$$

$$0 < p_{\max} \leq 0.09 \left[\frac{E(B-V)}{\mathrm{mag}}\right] \approx 0.03 \left[\frac{A_V}{\mathrm{mag}}\right] \approx 0.03\tau_V$$

[Fig 4.7, Whittet, Dust in the Galactic Environment]

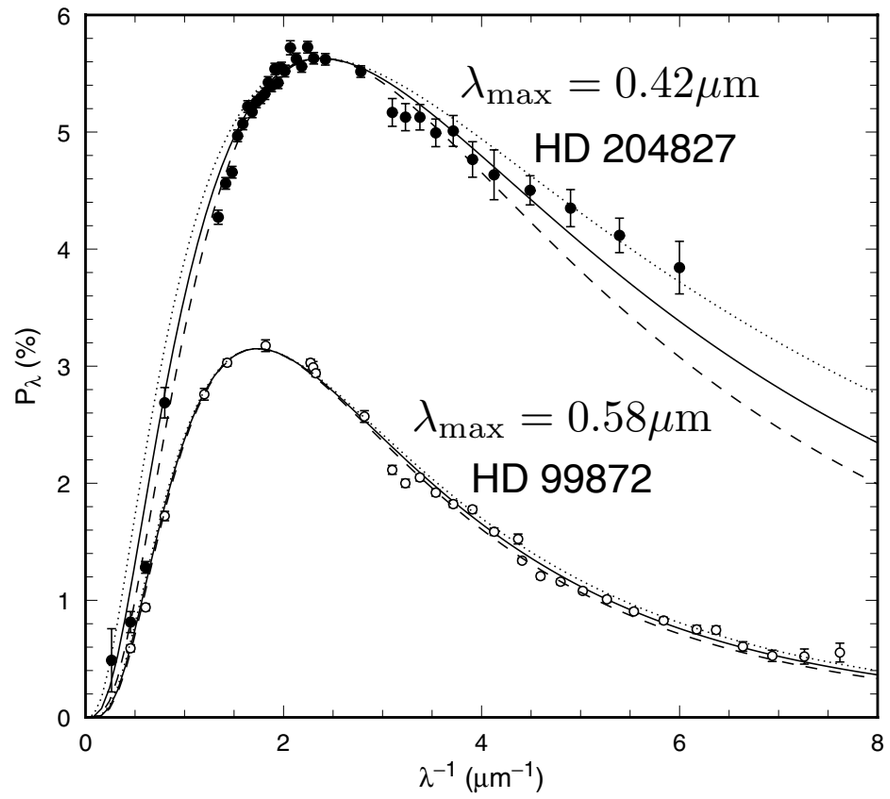

- The reason that the light becomes polarized is that some fraction of the dust grains are elongated and that their long axes line up in the same direction. When they do, the light is slightly more blocked along the long axis of the grains than along the short axis - and polarization results.
- The polarization is produced by dust grains that are somewhat partially aligned by the interstellar magnetic field. The grains are appeared to be aligned with their shortest axes tending to be parallel to the magnetic field direction.
- The decline of polarization towards the UV reflects that small grains apparently do not contribute appreciably to the polarization, either because they are more spherical or because they are not well aligned.

- ***Polarized Infrared Emission***
  - The far-IR emission from aligned dust grains will also be polarized, this time with a direction along the long axis of the grains. Far-IR polarization has been observed for a large number of molecular clouds that have “high” dust emission optical depths at long wavelengths (~ 0.1-1 mm).
- ***Polarization due to scattering***
  - Scattering of light by dust grains generally also lead to polarization.
  - For single scattering, the polarization vector is perpendicular to the line connecting the light source and the scattering grain.
  - The degree of polarization and its distribution provide information on the characteristics of the scattering grains and the geometry of the nebula.

Linear polarization of the IR reflection nebula associated with the region of massive star formation in Orion. The linear polarization vectors measured at K are superimposed on a map of the scattered light intensity.

[Werner et al. 1983, ApJ, 265, L13]

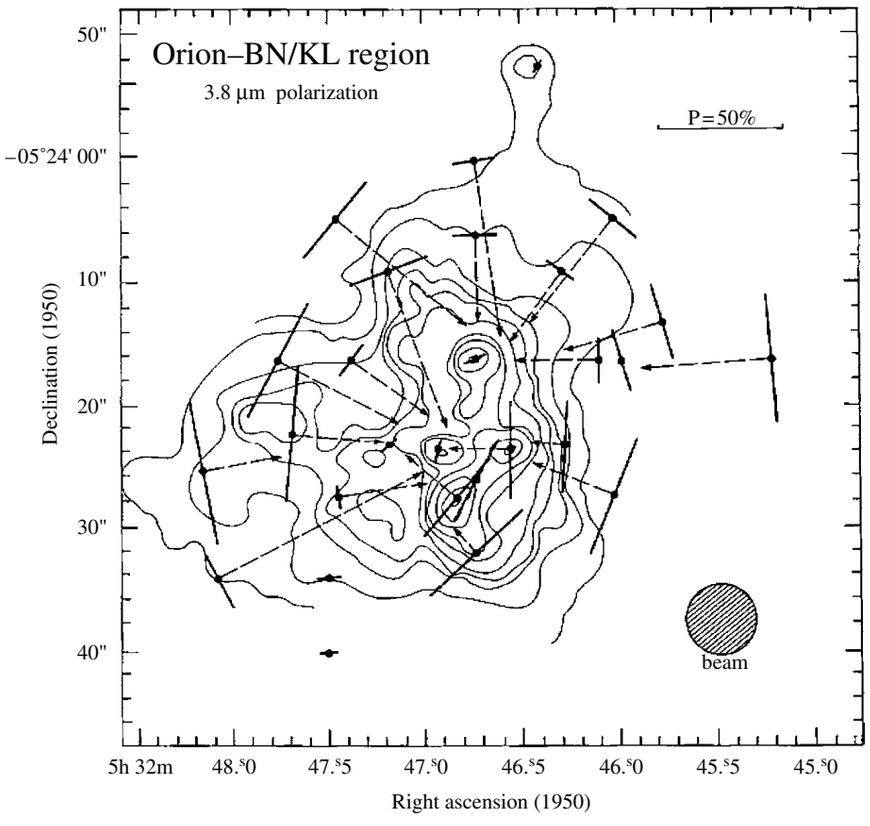

Luminescense

- ***Extended Red Emission (ERE)***
  - Many dusty objects — including the diffuse ISM, dark clouds, reflection nebulae, post-AGB objects, planetary nebulae, HII regions, and starburst galaxies — show a broad ($\Delta\lambda$ = 600-1000Å), featureless emission band in the red part of the spectrum (6000-8000Å). This is called extended red emission (ERE).
  - The ERE cannot be due to thermal emission but rather represents a luminescence process whereby an absorbed UV or visible photon is down-converted to the ERE range.
  - Various forms of carbonaceous materials and crystalline silicon nanoparticles have been proposed as carries of ERE. In particular, Witt et al. (1998) and Ledoux et al. (1998) suggested ***crystalline silicon nanoparticles with 15-50Å diameters*** as the carrier on the basis of experimental data showing that silicon nanoparticles could provides a close match to the observed ERE spectra and satisfy the quantum efficiency requirement.

- What is (photo)luminescence?
  - ***Luminescence*** (냉광) is any emission of light from a substance that does not arise from heating. ***Incandescence*** (백열광) is light emission due to the elevated temperature of a substance, such as a glowing hot ember.
  - ***(Photo)luminescence*** is the emission of light from a material following the absorption of light (photo-excitation).
  - ***Fluorescence*** (형광) is prompt (photo)luminescence that occurs very shortly after photo-excitation of a substance, while ***phosphorescence*** (인광) is long-lived (photo)luminescence that continues long after the photo-excitation has ceased.

Infrared Emission

- ***Infrared Emission***
  - Dust grains are heated by starlight, and cool by radiating in the infrared.
  - Along a typical line of sight through our galaxy, the ratio of dust IR emission to the hydrogen column density tells us the IR luminosity per hydrogen nucleus:

$$\frac{I_{\rm IR}}{N_{\rm H}} = 5 \times 10^{-24}\,{\rm erg\,s^{-1}}$$

  - The IR spectrum provides very strong constraints on grain models.
  - There are two components: ***a cold (T ~ 15-20 K) component*** emitting mainly at long wavelengths (far-IR) and ***a hot (T ~ 500 K) component*** dominating the near- and mid-IR emission.
    - The cold component is due to large dust grains in radiative equilibrium with the interstellar radiation field.
    - The hot component is due to ultra small grains and PAH species that are heated by a single UV photon to temperatures of ~ 1000 K and cool rapidly in the near- and mid-IR.

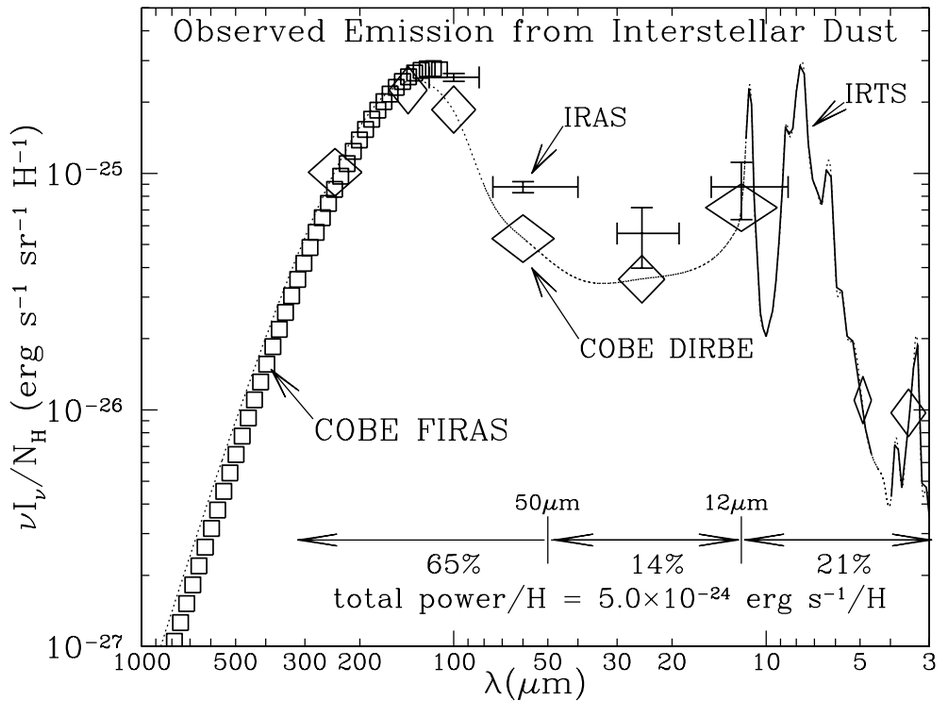

Observed IR emission per H nucleon from dust heated by the average starlight background in the local Milky Way.

[Fig 21.6 Draine]

What are the dust grains made of?

- Observational Constraints
  - **Interstellar Depletion**: Certain elements appears to be underabundant or "depleted" in the gas phase. The observed depletions tell us about the major elemental composition of interstellar dust.

  - **Spectroscopy**: We would observe spectroscopic features that would uniquely identify the materials, and allow us to measure the amounts of each material present. But, it is difficult to apply this approach to solid materials because: (1) the optical and UV absorption is largely a continuum; and (2) the spectral features are broad, making them difficult to identify conclusively.

  - **Extinction**:
    - The wavelength dependence of the extinction curve provides constraints on the interstellar grain size distribution.
    - What materials could plausibly be present in the ISM in quantities sufficient to account for the observed extinction? A Kramers-Kronig integral over the observed extinction indicates that the total grain mass relative to total hydrogen mass:

$$M_{\rm dust}/M_{\rm H} \gtrsim 0.0083$$

Interstellar Depletion

- Condensible elements:
  - Hydrogen: There is no way to have hydrogen contribute appreciably to the grain mass (even polyethylene $(CH_2)_n$ is 86% carbon by mass).
  - The noble gases (He, Ne, Ar, Kr, Xe…) and nitrogen(N), zinc (Zn), and sulfur (S) are examples of species that generally form only rather volatile compounds. They are observed to be hardly depleted at all.
  - The only way to have a dust/H mass ratio of 0.0056 or higher is to build the grains out of the most abundant condensible elements: C, O, Mg, Si, S, and Fe (refractory materials; 내열성물질).

- Abundance Constraints toward ζ Oph
  - Nitrogen is present at its solar abundance.
  - C abundance is at ~ 35% of its solar value.
  - O abundance is at ~ 55% of its solar value.
  - Mg is at ~ 11%.
  - Si is at ~ 5%.
  - Fe is at ~ 0.4%.

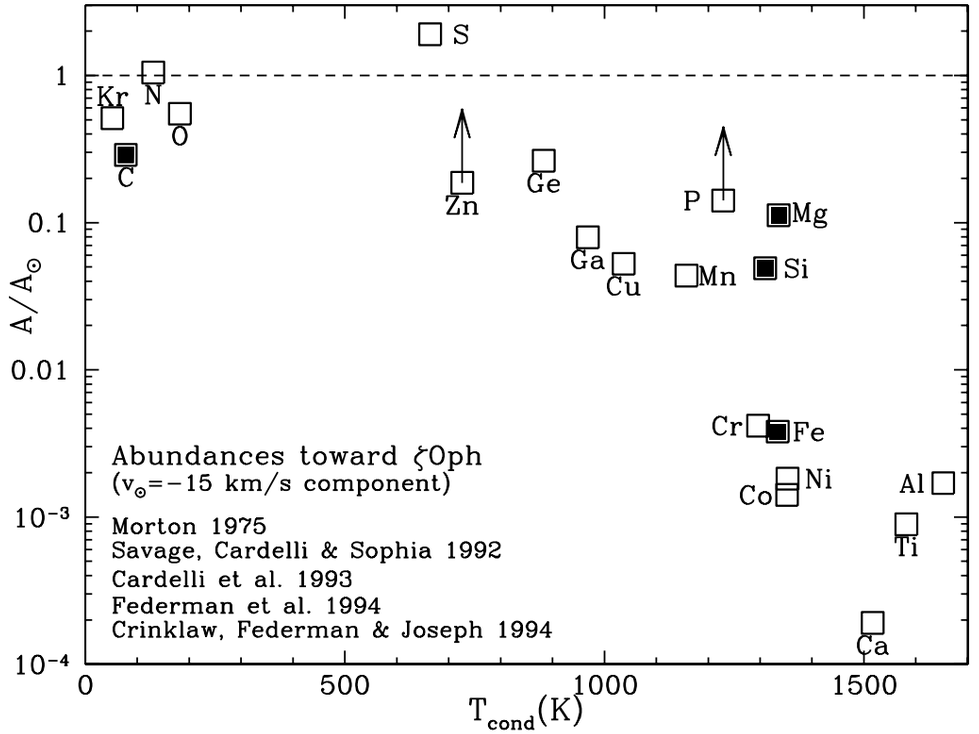

Gas-phase abundances (relative to solar) in the diffuse cloud toward ζ Oph, plotted versus "condensation temperature"

Gas-phase abundance vs. Condensation Temperature

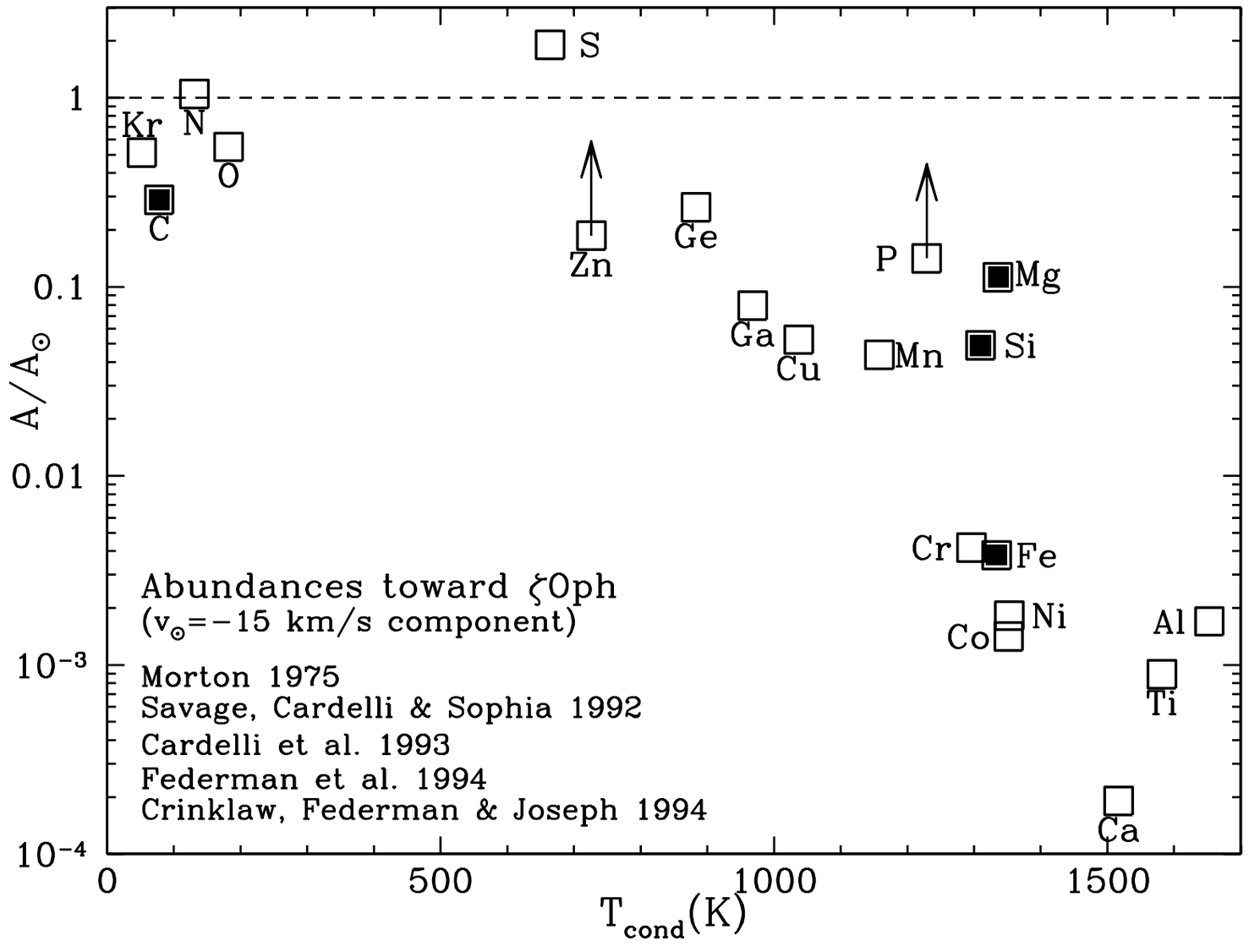

Figure 23.1 in [Draine]

Gas-phase abundances (relative to solar) in the diffuse cloud toward ζ Ophiuchi (O9.5V star, 138 pc), plotted versus "condensation temperature". Solid symbols: major grain constituents C, Mg, Si, Fe. The apparent overabundance of S may be due to observational error, but may be arise because of S II absorption in the H II region around ζ Oph. There's a strong tendency for elements with high T_{cond} to be under abundant in the gas phase, presumably because most of the atoms are in solid grains.

Condensation temperature : temperature at which 50% of the element in question would be incorporated into solid material in a gas of solar abundances, at LTE at a pressure $p = 10^2$ dyn cm^{-2} (Lodders 2003).

- With the elements providing the bulk of the grain volume identified, we can limit consideration to the following possible materials:
  - Silicates
    - pyroxene composition $\mathrm{Mg_xFe_{1-x}SiO_3}\ (0 \leq \mathrm{x} \leq 1)$
    - olivine composition $\mathrm{Mg_{2x}Fe_{2-2x}SiO_4}\ (0 \leq \mathrm{x} \leq 1)$
  - Oxides of silicon, magnesium, and iron (e.g., SiO_2, MgO, Fe_3O_4)
  - Carbon solids (graphite, amorphous, and diamond)
  - Hydrocarbons (e.g., polycyclic aromatic hydrocarbons)
  - Carbides, particularly silicon carbide (SiC)
  - Metallic Fe
  - Other elements (e.g., Ti, Cr, Al, and Ca) are also present in interstellar grains, but because of their low abundances, they contribute only a minor fraction of the grain mass.

Extinction Curve - The sizes of Interstellar Grains

- The extinction keeps rising throughout the IR, visible and near- and far-UV wavelength range.
  - ***Babinet's theorem***: Since extinction "saturates" when the grain size becomes comparable to or bigger than the wavelength ($a \gtrsim \lambda$), interstellar grains have to span a range of sizes.
  - ***Mie theory***: The extinction at wavelengthλ is mainly due to a grain size $a \sim \lambda/2\pi$.
    - The visible extinction is then due to grains with a typical size of 2000Å.
    - The UV extinction, on the other hand, reflects the presence of grains with sizes in the range of 50-200Å.

- Size of dust grains:

$$\frac{A_V}{N_{\rm H}} = 1.086\frac{\tau_V}{N_{\rm H}} = 1.086\frac{n_{\rm d}C_{\rm ext}(\lambda_V)}{n_{\rm H}}$$

assuming $C_{\rm ext} \approx \pi a^2$ $\Longrightarrow$

$$\frac{A_V}{N_{\rm H}} \approx 5.3\times10^{-22}\,{\rm mag\,cm^2\,H^{-1}}$$

$$\frac{n_{\rm d}(a)}{n_{\rm H}} \approx \frac{A_V/N_{\rm H}}{1.086(\pi a^2)} \approx \frac{4.88\times10^{-22}}{\pi(a/{\rm cm})^2}$$

- Ascribing the observed visual extinction per H to ~ 2000Å grains implies an abundance of such grains of ~ 4×10^{-13}.
- Similarly, the 10 times higher FUV extinction per H atom results in an abundance of ~ 100Å grains of 2×10^{-9}.

Observed Spectral Features of Dust

- The 2175Å Feature (UV bump)
  - The strongest feature in the interstellar extinction curve is a broad “bump” centered at ~ 2175Å where there is additional absorption above the rough 1/λ behavior at adjacent wavelengths.
    - The feature is well-described by a Drude profile.

$$S(\lambda) = \frac{2}{\pi} \frac{\gamma_0 \lambda_0 \sigma_{\rm int}}{(\lambda/\lambda_0 - \lambda_0/\lambda)^2 + \gamma_0^2} \quad \text{where } \sigma_{\rm int} = \int S(\lambda) d\lambda^{-1}$$

    - The central wavelength is nearly identical on all sightlines, but the width varies significantly from one region to another.
    - The strength of the feature is a strong function of the metallicity of the gas, with the UV bump appearing slightly weaker in the LMC extinction curve (metallicity ~ 50% solar), but essentially absent in the SMC extinction curve (metallicity ~10% solar).
  - The strength of this feature implies that the responsible material must be abundant: it must be made of H, C, N, O, Mg, Si, S, or Fe.
  - Small graphite grains would have a strong absorption peak at about this frequency, due to $\pi \Rightarrow \pi^*$ electronic excitations in the sp^2-bonded carbon sheets.
    - It seems most likely that the 2175Å feature is due to some form of sp^2-bonded carbon material.
    - This is generally attributed to particles rich in carbon, either in the form of graphite, hydrogenated amorphous carbon grains, or various aromatic forms of carbon, but models have not yet succeeded in reproducing all the details (the width of the feature).
  - Alternatives have been suggested. OH- on small silicate grains.

- Mid-Infrared Silicate Features:
  - There is a conspicuous IR absorption feature at 9.7μm. Silicate minerals generally have strong absorption responses due to the Si-O stretching mode near 10μm.
  - It seems virtually certain that the interstellar 9.7μm feature is due to silicates. This conclusion is strengthened by the fact that the 10μm emission feature is seen in the outflows from oxygen-rich stars (which would be expected to condense silicate dust) but not in the outflows from carbon-rich stars.
  - Near 18μm, interstellar dust shows another feature, attributable to the Si-O-Si bending mode in amorphous silicates.

The fact that the 9.7μm band is fairly featureless, unlike what is seen in laboratory silicate crystals, suggests that this “astrophysical” silicate is primarily amorphous rather than crystalline in nature.

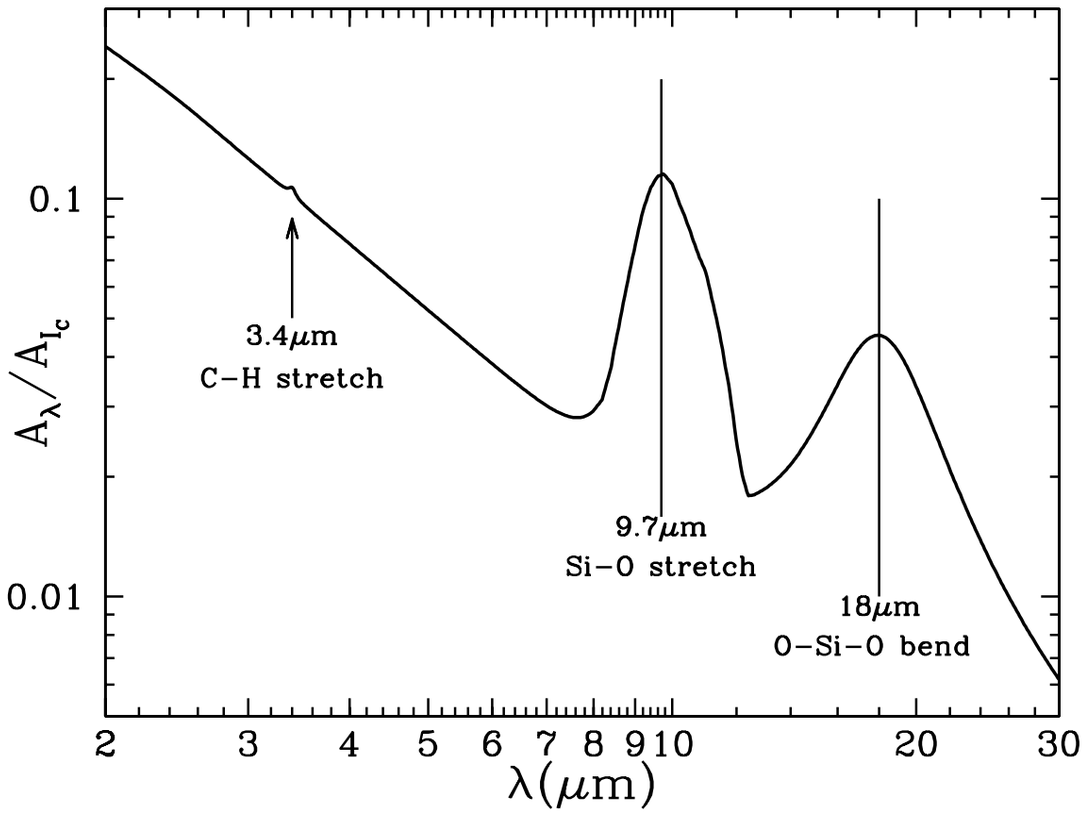

IR extinction curve.
[Fig 23.2 Draine]

- The 3.4μm Feature
  - There is a broad absorption feature at 3.4μm that is almost certainly due to the C-H stretching mode in “aliphatic” hydrocarbons (organic molecules with carbon atoms joined in straight or branched chains).
  - The 3.4μm C-H feature is found to be weaker (relative to the overall extinction) in dark clouds than in diffuse clouds (Shenoy et al. 2003), which has been interpreted as evidence that the C-H bonds responsible for the 3.4μm feature are destroyed in molecular clouds, perhaps as the result of cosmic ray irradiation, and regenerated when carbonaceous grains are exposed to atomic hydrogen in diffuse clouds.

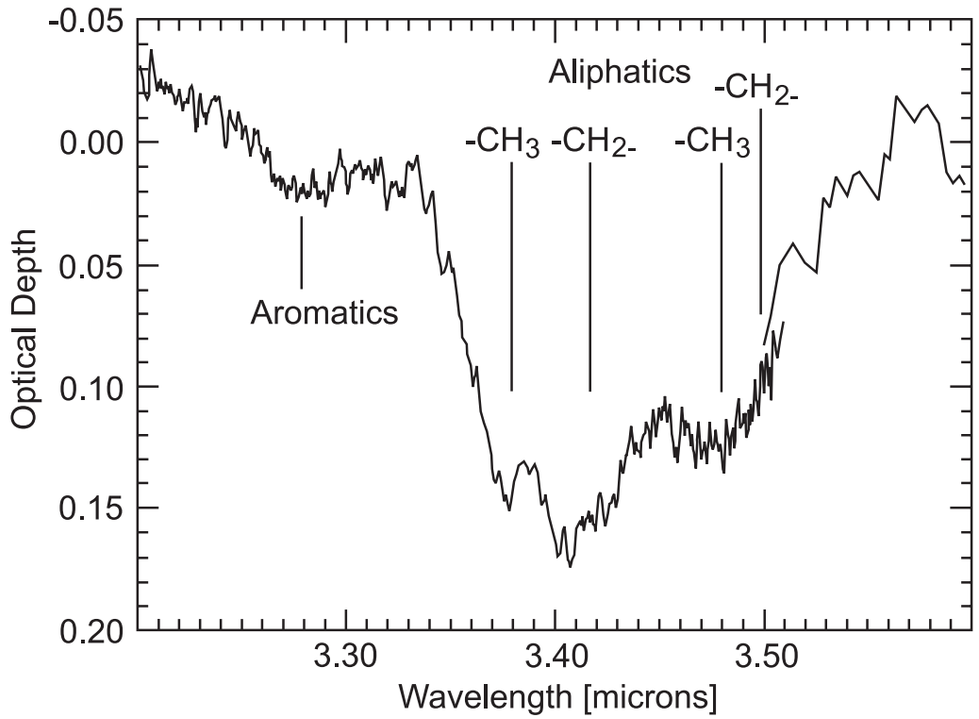

The source GCS3 in the Galactic Center
Chiar et al. (2000, ApJ)

- Aromatic/aliphatic ratio:
  - Pendleton & Allamandola (2002) concluded that the carbonaceous material was ~85% aromatic (ring) and ~15% aliphatic.
  - However, Dartois et al. (2004) concluded that at most 15% of the carbon is aromatic.
  - The aromatic/aliphatic ratio remains uncertain.

- Diffuse Interstellar Bands
  - There are numerous web, very broad (FWHM > 140Å) features, known as the diffuse interstellar bands or DIBs, at visible wavelengths.
  - These features are too broad to be absorption lines of atoms, ions, or small molecules. The strengths of DIBs are in general correlated with dust extinction, so it is likely that the DIBs are associated with the dust grain population.
  - The first DIBs were discovered 98 years ago (Heger 1922) and their interstellar nature was established 86 years ago (Merrill 1934).
  - ***However, not a single one of the DIBs has been convincingly identified!***

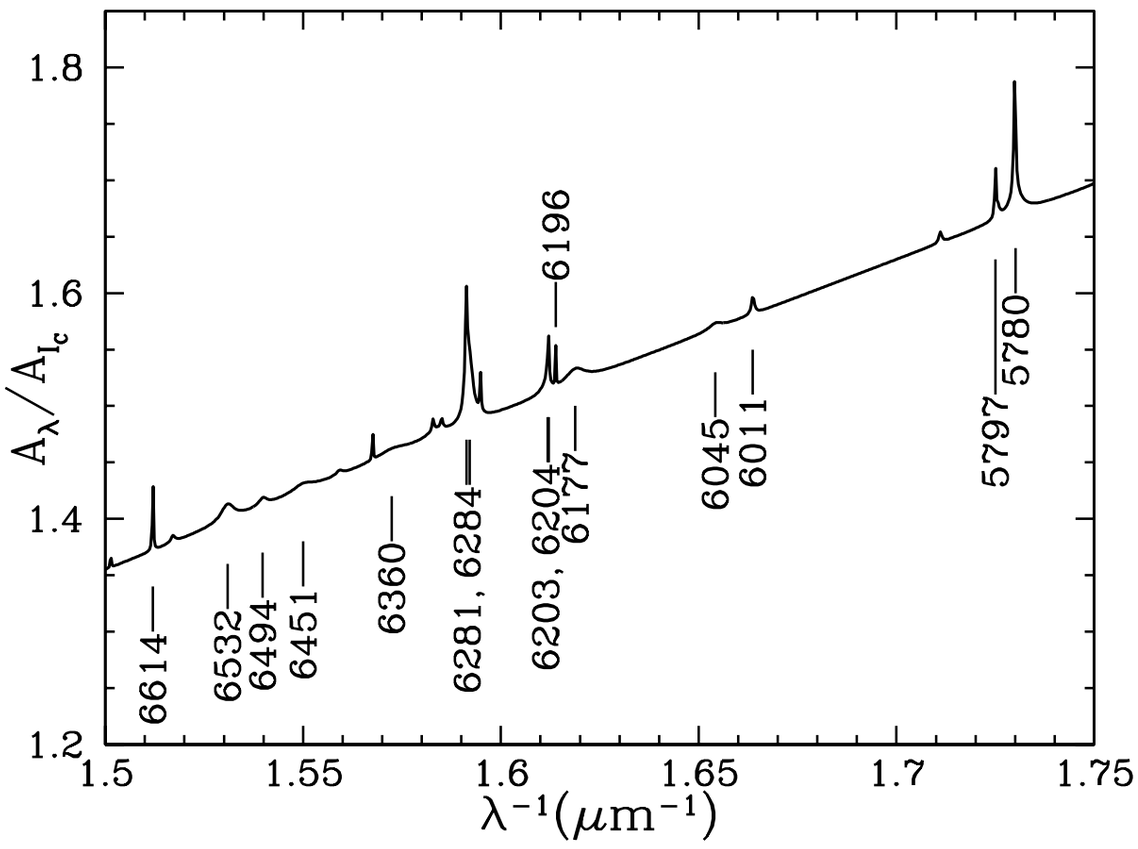

Some of the DIBs may be due to free-flying large molecules (i.e., ultrasmall dust grains).

Extinction curve, showing some of the DIBs

Fig 23.3 Draine

- Ice Features in Diffuse and Dark Regions
  - In dark molecular clouds, a number of absorption features appear, most notably a strong band at 3.1μm which is produced by the O-H stretching mode in H_2O ice.
  - A number of other absorption features are also seen, including features due to CO (4.67μm), CH_3OH (3.53μm, methanol), and CO_2 (15.2μm).
  - These are generally though to arise in icy “mantles” that encase dust grains found in dense molecular clouds. Ice mantles are not found on grains in the general ISM, as exposure to the interstellar radiation field sublimes the ices.
  - CO is a molecule most commonly observed in the gas phase, but it can condense as a “frost” onto dust grains when the temperature drops below ~ 17K. CO_2 has not yet positively observed in the gas phase (despite numerous searches) but it is seen as an ice condensed onto grains surfaces.

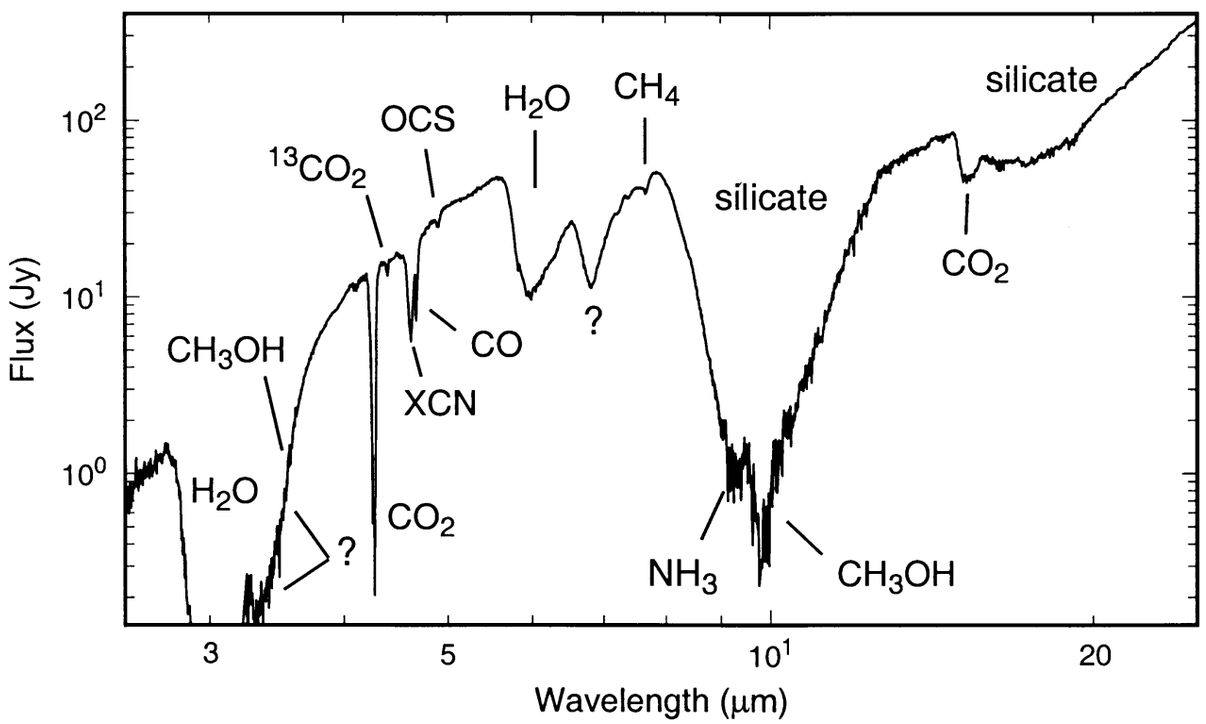

Spectrum of the dust-embedded young stellar object W33A.

An ice feature called XCN at 4.62μm is attributed to $\mathrm{C} \equiv \mathrm{N}$ bonds, but the “X” carrier is so far unidentified.

Gibb et al. (2000, ApJ)

The spectrum of a vibrational transition of a diatomic ***gas*** molecule, like CO, splits into rotational line which generally group into an R-branch and a P-branch corresponding to rotational transitions with $\Delta J = 1$ and $\Delta J = -1$, respectively.

Molecules in an ice mantle are squeezed in by other molecules and cannot rotate freely, so these branches are suppressed.

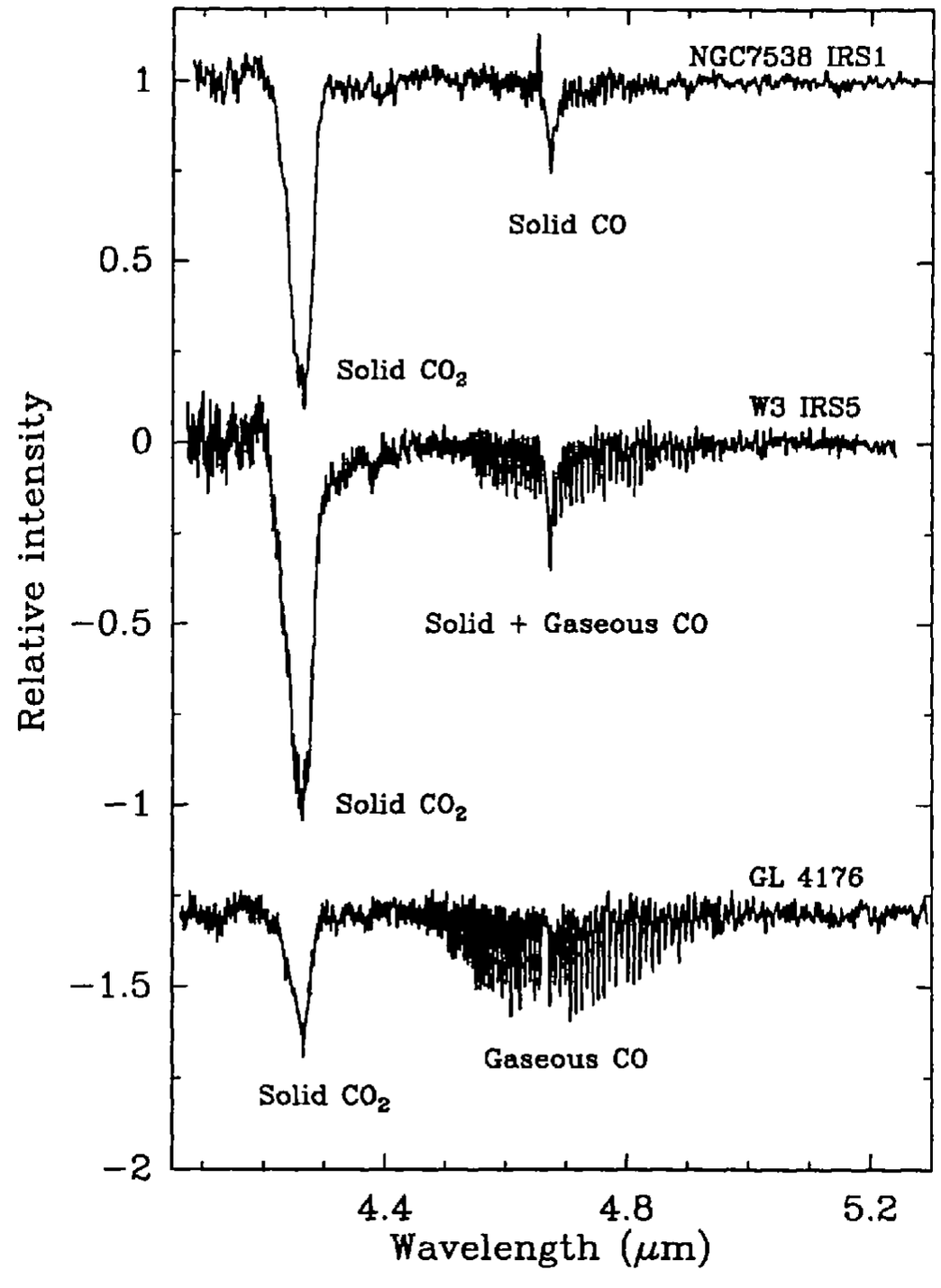

van Dishoeck et al. (1998, ASPC)

Homework (due date: 05/30)

[Q16]

From Ryden's book

Technologically advanced (but ethically dubious) space aliens have found a method of converting mass M to energy E with 100% efficiency, using Einstein's relation $E = Mc^2$.

(a) The star Proxima Centauri ($M_{\rm pc} = 0.123\,{\rm M}_\odot$, $R_{\rm pc} = 0.143\,{\rm R}_\odot$) is at a distance $d = 1.301$ pc from the Earth. The space aliens convert 5% of Proxima Centauri's mass into energy, and use that energy to eject the remaining 95% spherically outward at an initial speed $u_{\rm ej}$. What is $u_{\rm ej}$ in kilometers per second?

(b) The gas between the solar system and Proxima Centauri is part of the Local Interstellar Cloud, with mean density $n_{\rm H} = 1\,{\rm cm}^{-3}$ and temperature $T = 8000$ K. Assuming uniform density and temperature, how long will it take the blastwave from the explosion in part (a) to reach the solar system? If the aliens beam us a taunting radio message at the same time they blow up Proxima Centauri, how long will we have to prepare for the arrival of the blastwave?

(c) What will be the speed $u_{\rm sh}$ of the blastwave as it passes through the solar system?

(d) What will be the pressure P_2 and the temperature T_2 right behind the blastwave as it passes through the solar system?

(e) What will be the total thermal energy of the portion of the blastwave that strikes the Earth? Is this greater than or less than the thermal energy of the Earth's atmosphere? [Hint: in addition to knowing the Earth's radius and average atmospheric temperature, you will need to know the mass of its atmosphere.]